

Density Functional Theory (DFT) Investigation of Fullerene and Non-Fullerene donor part of Organic Photovoltaic cell



By

Muhammad Moazam Yaseen

(Registration No: 00000363597)

Department of Chemical Engineering

School of Chemical and Materials Engineering (SCME)

National University of Sciences and Technology (NUST)

Islamabad, Pakistan

(2024)

Density Functional Theory (DFT) Investigation of Fullerene and Non-Fullerene donor part of Organic Photovoltaic cell



By

M.Moazam Yaseen

(Registration No: 00000363597)

A thesis submitted to National University of Science and Technology, Islamabad,

in partial fulfillment of the requirement for the degree of

Master of Science in

Chemical Engineering

Supervisor: Dr. Umair Sikandar

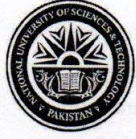
Co Supervisor: Dr Uzma Habib

School of Chemical and Materials Engineering (SCME)

National University of Sciences and Technology (NUST)

Islamabad, Pakistan

(2024)



THESIS ACCEPTANCE CERTIFICATE

Certified that final copy of MS Thesis entitled "Density Functional Theory (DFT) Investigation of Fullerene and Non-Fullerene Donor Part of Organic Photovoltaic Cell" written by Mr **Muhammad Moazam Yaseen** (Registration No 00000363597), of School of Chemical & Materials Engineering (SCME) has been vetted by undersigned, found complete in all respects as per NUST Statues/Regulations, is free of plagiarism, errors, and mistakes and is accepted as partial fulfillment for award of MS degree. It is further certified that necessary amendments as pointed out by GEC members of the scholar have also been incorporated in the said thesis.

Signature: _____

Name of Supervisor: **Dr Umair Sikandar**

Date: _____

Signature (HOD): _____

Date: _____

Signature (Dean/Principal): _____

Date: _____



National University of Sciences & Technology (NUST)

FORM TH-4

MASTER'S THESIS WORK

We hereby recommend that the dissertation prepared under our supervision by

Regn No & Name: 00000363597 Muhammad Moazam Yaseen

Title: Density Functional Theory (DFT) Investigation of Fullerene and Non-Fullerene Donor Part of Organic Photovoltaic Cell.

Presented on: 17 Oct 2024 at: 1500 hrs in SCME Seminar Hall

Be accepted in partial fulfillment of the requirements for the award of Master of Science degree in Chemical Engineering.

Examination Committee Members

Name: Dr Erum Pervaiz

Signature: [Signature]

Name: Dr Muhammad Ahsan

Signature: [Signature]

Name: Dr Uzma Habib (Co-Supervisor)

Signature: [Signature]

Supervisor's Name: Dr Umair Sikander

Signature: [Signature]

Dated: 14-11-24

[Signature]

15/11/24

Head of Department

Date

COUNTERSIGNED

Date _____

[Signature]
18/11/24
Dean/Principal

School of Chemical & Materials Engineering (SCME)

AUTHOR'S DECLARATION

This thesis, titled "Density Functional Theory (DFT) Investigation of Fullerene and Non-Fullerene Donor Parts of Organic Photovoltaic Cell," is entirely Muhammad Moazam Yaseen's original work and has not previously been submitted for a degree at any institution, including the National University of Sciences and Technology, Islamabad. I understand that the university retains the right to withdraw my MS degree if this statement is found to be incorrect, even after my graduation.

Student Name: M. Moazam Yaseen

PLAGIARISM UNDERTAKING

I solemnly declare that the research work presented in the thesis titled "Density Functional Theory (DFT) Investigation of Fullerene and Non-Fullerene Donor Part of Organic Photovoltaic Cell" is entirely my own. While any minor contributions or assistance received have been duly acknowledged within the thesis, the complete work, from research to writing, was independently authored by me.

In accordance with the National University of Sciences and Technology (NUST), Islamabad and the Higher Education Commission (HEC) policies on academic integrity, I, the author of the thesis titled "Density Functional Theory (DFT) Investigation of Fullerene and Non-Fullerene Donor Part of Organic Photovoltaic Cell," confirm that all sources and references are properly cited within the work.

I understand that the National University of Sciences and Technology (NUST), Islamabad and the Higher Education Commission (HEC) have established policies regarding academic integrity. Should any violation of these policies be identified in my thesis, titled "Density Functional Theory (DFT) Investigation of Fullerene and Non-Fullerene Donor Part of Organic Photovoltaic Cell," even after the award of my MS degree, I acknowledge the university's right to take appropriate action.

Name: M. Moazam Yaseen

This accomplishment wouldn't be possible without the unwavering support and cooperation of my incredible parents and my loving family. To them, with all my love.

ACKNOWLEDGMENT

"And He found you lost and guided [you]. And He found you poor and made [you] self-sufficient. So as for the orphan, do not oppress [him]. And as for the petitioner, do not repel [him]. But as for the favor of your Lord, report [it]." (Surah Adh-Dhuha, 93:7-11)

I express profound gratitude to the **Almighty Allah**, the Most Compassionate, for endowing me with the capacity, comprehension, and direction to successfully accomplish this research work as a prerequisite for my master's degree. I would want to express my gratitude to Allah and the direction of the holy prophet **Muhammad SAW**, without whom this job would not have been accomplished.

Dear Supervisor [**Dr. Umair Sikandar**],

I am writing to express my sincere gratitude for your guidance and support throughout the process of completing my Master's thesis, titled "[Comparison b/w Fullerene and Non-Fullerene donor part of Organic Photovoltaic cells- a DFT study]." Your expertise, encouragement, and invaluable feedback have been instrumental in shaping the direction of my research and enhancing the overall quality of my work.

I would like to extend my appreciation to my Co-Supervisor, [**Dr. Uzma Habib, SINES**] and other GC members for their insightful comments and constructive acclamation. Their diverse perspectives have enriched the depth of my study and provided valuable insights that significantly contributed to the refinement of my thesis.

Lastly, I owe a debt of gratitude to my family for their unwavering support, patience, and understanding. Their encouragement and belief in my abilities have been the driving force behind my academic accomplishments.

Thank you once again for your mentorship and support. I am truly grateful for the opportunities and knowledge gained during this academic pursuit.

Thanks a lo

TABLE OF CONTENTS

ACKNOWLEDGEMENTS	VIII
List of Figures	XII
List of Tables	XIII
List of Symbols, Abbreviations	XIV
1 CHAPTER 1: INTRODUCTION.....	1
1.1 Background of Photovoltaic Cell:	1
1.2 Recent Commitments and Objectives:	2
1.3 Photovoltaic System for power generation:	3
1.4 PV Cells' underlying structure:	4
1.4.1 Semiconductor layers.....	5
1.4.2 Conducting materials	5
1.4.3 Anti-reflecting coating	5
1.5 Types of Solar Cells:	5
1.5.1 Amorphous Silicon Solar Cell (A-Si).....	6
1.5.2 Biohybrid Solar Cell	6
1.5.3 Buried Contact Solar Cell	7
1.5.4 Cadmium Telluride Solar Cell (CdTe)	7
1.5.5 Concentrated PV Cell (CVP and HCVP).....	8
1.5.6 Copper Indium Gallium Selenide Solar Cells (CI (G) S):	8
1.5.7 Dye-Sensitized Solar Cell (DSSC)	9
1.5.8 Gallium Arsenide Germanium Solar Cell (GaAs)	9

1.5.9	Hybrid Solar Cell	11
1.5.10	Luminescent Solar Concentrator Cell (LSC).....	12
1.6	Why Organic Materials?:	12
1.7	Varieties of Organic Solar Cell Device Structures:	13
1.7.1	Organic single-layer solar cell	13
1.7.2	Organic Double Layer Solar Cell	14
1.7.3	Bulk heterojunction (BHJ) organic solar cell	14
1.8	Materials for organic photovoltaics (OPV):.....	15
1.8.1	Electron-donor materials.....	16
1.8.2	Electron-acceptor materials	17
1.8.3	Donor-acceptor polymer	18
1.8.4	Electron donor-acceptor-donor (D-A-D)	18
1.9	Computational Studies:	19
1.9.1	Classical Mechanical Methods	19
1.9.2	Molecular Mechanics (MM).....	20
1.10	Quantum Mechanical Methods:	20
1.10.1	Ab- initio method.....	20
1.10.2	Semi-Empirical method	20
1.10.3	Density functional theory (DFT) method	21
CHAPTER 2: LITERATURE REVIEW		23
2.1	Historical background of Photovoltaics:	23
2.2	Organic Photovoltaic Cells:	25
2.3	Organic Materials in PV Cells:	26
2.3.1	Donor Materials	26
2.3.2	Acceptor Materials.....	28

2.3.3	Donor-Acceptor materials.....	29
2.3.4	Donor-Acceptor-Donor.....	31
2.3.5	Goals and Purposes:.....	32
CHAPTER 3: METHODOLOGY		34
3.1	Molecular Modelling:.....	34
3.1.1	GaussView06	35
3.2	Gaussian-09:.....	35
3.3	Density functional theory (DFT):.....	36
3.3.1	Geometry Optimization	37
3.3.2	B3LYP functional	37
3.3.3	6-311G Basis set	37
3.3.4	Time-Dependent Self-Consistent Field.....	38
3.4	Description of Structures:.....	39
4	CHAPTER 4: RESULTS.....	42
4.1	Molecular Modeling.....	42
4.2	Geometry optimization.....	43
4.3	Electronic properties	46
4.4	Electronic Transition and Absorption spectra.....	48
4.5	Photovoltaic properties.....	51
4.5.1	Voc:.....	51
4.5.2	α (ΔE).....	52
5	CHAPTER 5: DISCUSSION	55
6	CHAPTER 6: CONCLUSION	59
7	REFERENCES	60

LIST OF FIGURES

Figure 1-1 Block Diagram of typical photovoltaic system [21]	4
Figure 1-2 Primary components of a PV cell [22]	4
Figure 1-3 Graphic showing the five layers that comprise CIGS solar cells [32]	9
Figure 1-4 Structure of carbon nanotubes based solar cells [32]	11
Figure 1-5 Organic Single-layer Solar Cell [49]	14
Figure 1-6 Bulk heterojunction (BHJ) [50]	15
Figure 1-7 Examples of electron-donor materials [61]	17
Figure 1-8 Examples of electron-acceptor materials [63]	18
Figure 2-1 Oil Crisis [84]	24
Figure 2-2 Working mechanism of OPVs [115]	32
Figure 3-1 Methodology Flow chart of Computational Modelling	34
Figure 3-2: Structures based on C60 attached group	39
Figure 3-3: Structures based on Pentacene attached group	40
Figure 3-4: Structures based on 2H-benzo[cd]pyrene attached	40
Figure 4-1: Structure of Basic Molecule	43
Figure 4-2: Optimized Structure of C60 attached molecule	44
Figure 5-1: Reference Molecule	55

LIST OF TABLES

Table 3-1: Classifications of Structures	41
Table 4-1 The Energy value of Optimized Geometries of C60	45
Table 4-2 The Energy value of Optimized Geometries of Pentacene	45
Table 4-3: The Energy value of Optimized Geometries of 2H-benzo[cd]pyrene	45
Table 4-4: HOMO-LUMO Energy values and Energy gap values of C60 structures	47
Table 4-5: HOMO-LUMO Energy values and Energy gap values of Pentacene attached structures	47
Table 4-6: HOMO-LUMO Energy values and Energy gap values of 2H-benzo[cd]pyrene attached structures	48
Table 4-7: The Excitation Energy, Absorption λ_{\max} (nm), Oscillator strength (O.S) of C60 structures	49
Table 4-8: The Excitation Energy, Absorption λ_{\max} (nm), Oscillator strength (O.S) of Pentacene attached structures	50
Table 4-9: : The Excitation Energy, Absorption λ_{\max} (nm), Oscillator strength (O.S) 2H-benzo[cd]pyrene attached structures	50
Table 4-10: Showing the relationship of HOMO, LUMO, energy gap, Voc and α C60 structure	52
Table 4-11: Showing the relationship of HOMO, LUMO, energy gap, Voc and α of Pentacene attached structures	53
Table 4-12: Showing the relationship of HOMO, LUMO, energy gap, Voc and α of 2H-benzo[cd]pyrene attached structures	54

LIST OF ABBREVIATIONS

OSCs	Organic solar cells
PV	Photovoltaic
CdTe	Cadmium telluride
CIGS	Copper Indium Gallium Selenide
GaAs	Gallium arsenide
PSC	Polymer solar cell
DSSCs	Dye-sensitized solar cells
OPV	Organic photovoltaic
E_g	Bandgap
DFT	Density functional theory
MD	Molecular Dynamics
HOMO	Highest occupied molecular orbital
LUMO	Lowest unoccupied molecular orbital
O.S	Oscillator strength
V_{oc}	Open circuit voltage
$\alpha (\Delta E)$	Optimal energy difference

ABSTRACT

The transformation of solar energy into electrical energy via photovoltaic cells is presently regarded as one of the most exhilarating research endeavors. Organic photovoltaic (OPV) cells are in high demand for photovoltaic applications because of their mechanical flexibility, affordability, ease of production, and lightweight nature. The research has primarily focused on D-A-D (Donor-Acceptor-Donor) photovoltaic cells, extensively investigating the nature of Donor 1, Acceptor, and Donor 2 units.

In the context of this research, Density Functional Theory (DFT) in conjunction with Total Deposition Spectroscopy (TD-SCF) calculations utilizing the selected hybrid B3LYP-6311(G) functional is utilized to explore the electronic structure and properties of the reference material, with a focus on the examination of the properties resulting from the attachment of both fullerene and non-fullerene units at the first donor part. The research begins with the involvement of one fullerene unit in a reference molecule and exploring their molecular geometries, electronic band structures, and charge transport properties. Then two fullerene units were attached to compare their properties with the previous one. Similarly, the effect of non-fullerene aromatic units (Pentacene, 2H-benzo[cd]pyrene) was also studied by attachment of one and two units respectively. At the end, electron-donating alkyl groups (Methyl, Ethyl and Propyl) were attached to the acceptor part of the reference molecule in the presence of aromatic (fullerene, non-fullerene) units at 1st donor. A total number of 16 geometries were made and studied accordingly.

The results showed that when only one fullerene units was involved in the absence of alkyl groups, it possesses lowest energy band gap (0.31eV) compared to others and surpassed in exhibiting the best photovoltaic properties because a smaller energy gap is required for the easy excitation of electron from HOMO to LUMO and allows for a larger built-in potential across the device and leading to higher voltages across photovoltaic cell.

Results also indicate that attachment of two fullerene units in the absence of alkyl groups shows maximum λ value with ($\lambda_{\max} = 10982$ nm) and lowest value of excitation energy (0.113eV), while single fullerene unit has wavelength ($\lambda = 9960$ nm) and value of excitation energy

(0.125eV). By further proceeding, the molecule where ethyl group is attached as acceptor following the two fullerene units at 1st donor have maximum value of Voc (~1.787eV.)

In conclusion single C60 molecule with the donor part when no alkyl group is attached is more favorable than other molecules having non-fullerene aromatic compounds due to having very less amount of energy band gap.

CHAPTER 1: INTRODUCTION

Renewable energy resources have been attracting more attention lately as people become increasingly aware of the constrained availability of fossil fuels and the harmful effects of CO₂ and other greenhouse gas emissions [1]. One commonly used technique involves photovoltaics, which harness the photovoltaic effect to transform solar energy into electricity. In the field of photovoltaics, major kinds that can be distinguished as inorganic and organic. Over the last several decades, significant advancements have been made in the field of inorganic solar panels. The initial functional solar panel utilized silicon wafer and entirely inorganic materials throughout its construction. The materials commonly used in traditional photovoltaic cells include silicon (Si), gallium arsenide, cadmium-telluride (CdTe), and various compounds like copper-indium-gallium-diselenide and copper-zinc-tin-sulfide [2]. Over time, there has been a major expansion in the PCE of silicon solar cells, going from 10% to 26% [3]. Despite the progress made, there are still several drawbacks associated with inorganic photovoltaic cells. These include the use of costly materials, potential harm to the environment, the need for large and cumbersome panels, a significant initial investment required for commercialization, and complex production processes [2].

Over the last ten years, there has been a significant growth in interest and research focused on organic photovoltaic cells. The newfound interest is driven by two recent advancements in the organic semiconductor industry. Initially, it has been demonstrated that the quantum efficiency of electron transfer from an excited polymer to C₆₀ is exceptionally high, and the transfer occurs with remarkable speed [4]. This shows great potential for enhancing carrier separation in photovoltaic cells. Furthermore, the progress in creating effective organic displays using organic light emitting devices (OLEDs) has demonstrated the feasibility of organic electronic components. The displays are made with cheaper technology that can also be tested to create solar panels [5].

1.1 Background of Photovoltaic Cell:

A key method to transform sunlight into electrical power happens through the photovoltaic effect, which was initially noticed by Alexandre Edmond Becquerel in 1839 [6]. During the

electrochemical experiments, he recognized the occurrence of this effect on silver and platinum electrodes exposed to sunlight [7]. In the year 1905, Albert Einstein first up the idea of the photoelectric hypothesis. It discusses the connection between light waves and photons, which are the basic particles of light, along with the link between the energy of photons and their frequency (a direct relationship, with the ratio being the one linked to Planck's law). "In one of several epoch-making studies beginning in 1905, Albert Einstein explained that light consists of quanta—packets" with set energy matching to certain frequencies. In 1921, The Nobel prize was given to Einstein for his contributions to the field of physics, for a photon, which is a type of light quantum, to be able to release an electron, it must first possess a particular minimum frequency [8]. When silicon was substituted for selenium, it was found that very high efficiencies were realized. Russell Ohl is credited with identifying both the n-type and p-type zones within silicon in 1939. Additionally, he found the photoelectric effect within the p-n junctions [9]. It was in the year 1955 when a solar cell was installed in Americus, Georgia, to serve as the power source for a telecommunications network. Nearly one year following its introduction at the yearly gathering of the United States National Academy of Sciences, occurring in Washington on April 25, 1954, this marks the debut of the very first use of a solar cell. Furthermore, the concept of a photovoltaic system has expanded beyond just the solar cells to include additional components such as inverters, batteries, and even the necessary cables for connecting these elements. Each development in these devices increases in system's efficiency, hence amplifying the benefits of photovoltaic technology [10], [11].

1.2 Recent Commitments and Objectives:

Photovoltaic technology has shown to be more effective than anticipated recently. Printed photovoltaic panels are commonplace. There has been a decline in manufacturing costs due to the mass production of some technology. Now, photovoltaic panels are so readily available for use in public applications that the question that has to be answered is not how to generate energy (as in the 1990's), but rather how to generate energy that is environmentally friendly. This indicates that the energy that is produced ought to have a reduced ecological impact in contrast to any other method of producing it (often in comparison with sources of fossil fuels) [12], [13], [14]. To address the pressing issue of climate change and meet the growing energy demands of our society, a significant shift towards renewable energy sources is necessary [15].

In its proposed European Green Deal, the European Commission outlined ambitious goals to reduce greenhouse gas emissions by at least 55% by 2030 and achieve carbon neutrality by 2050 [15]. In 2015, the United Nations launched the Sustainable Development Goals (SDGs) via a publication known as "Transforming our world: the 2030 Agenda for Sustainable Development."

One method to illustrate the transformative potential of solar energy is by reviewing these aims. Among the 17 aims, solar energy is in harmony with three: The 7th aim provides clean and affordable energy, whereas the 11th aim focuses on creating sustainable cities and communities. Furthermore, the 13th aim stresses the need for immediate action regarding climate change [16].

1.3 Photovoltaic System for power generation:

Figure 1 illustrates a fundamental photovoltaic setup connected to the main power grid. This system converts energy from the sun into direct current (DC) electricity, with the intensity of sunlight directly affecting this process. A diode specifically designed to prevent power flow backward, permits the electricity produced by the photovoltaic system to be channeled solely into the power conditioning unit.

In the absence of a blocking diode, the battery might recharge into the solar panel during periods of minimal sunlight. The power conditioner comprises a Maximum Power Point Track (MPPT), a battery regulator, and a reverse current regulator [17], [18]. The MPPT optimizes the power generated by the solar PV array, always extracting the maximum amount. Meanwhile, the charge-discharge controller ensures that the battery bank is not overcharged or over-discharged, which is crucial for storing the electricity generated by solar energy during periods without sunlight. In simple PV setups, where the PV module's voltage matches the battery's, employing MPPT electronics is often considered superfluous. This is because the battery voltage stays consistent enough to effectively gather the highest possible power from the PV module. The system operates independently, not linked to the power grid [19], [20].

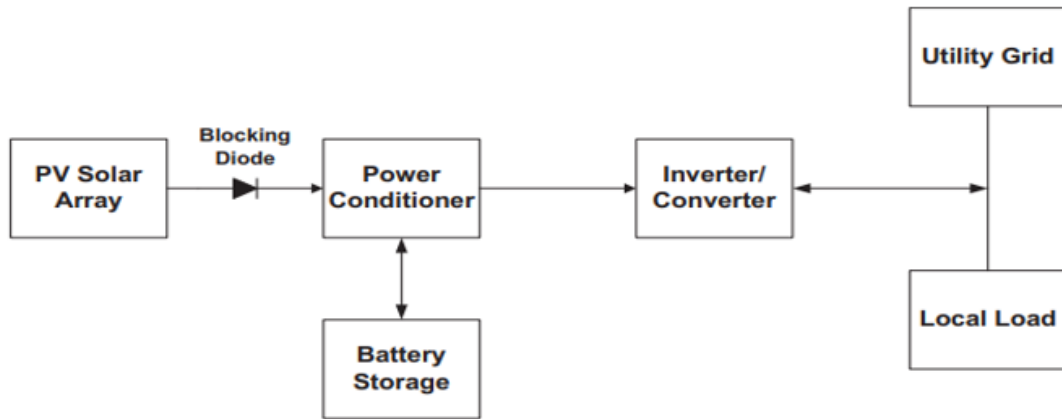


Figure 1-1 Block Diagram of typical photovoltaic system [21]

1.4 PV Cells' underlying structure:

Photovoltaic cells, often known as solar cells, are specialized devices that are meant to convert sunlight into electrical energy by utilizing the photovoltaic effect. Solar cells are also commonly referred to as photovoltaic cells. PV cells are the most fundamental component of photovoltaic (PV) systems [21]. Main components Are as follow;

- Semiconductor layers
- Conducting materials
- Anti-reflecting coating

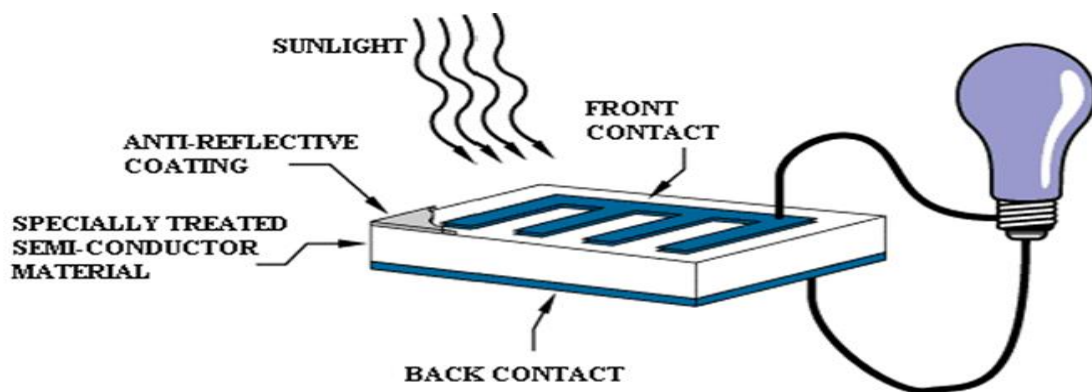


Figure 1-2 Primary components of a PV cell [22]

1.4.1 Semiconductor layers

As a result of its ability to effectively absorb and convert sunlight into electrical current through the process of photovoltaic effect, the semiconductor layer, which is also referred to as the absorber or active layer, is an essential component of a solar cell. Solar cells are made up of two unique layers of semiconductors, the N-type semiconductor layer, which is also referred to as the emitter, and the P-type semiconductor layer, which is known as the base. The P-N junction is formed as a result of the sandwiching of these two layers because of the sandwiching.

1.4.2 Conducting materials

Above the semiconductor layer is a conductive substance, which is often a thin layer of metal because of its electrical properties. The electron-hole pairs that are leaving the solar cell are able to leave more easily thanks to this layer. Solar cells lacking a conductive substance on their upper surface are unable to generate an electric current because they lack the ability to conduct electricity.

1.4.3 Anti-reflecting coating

An anti-reflective coating is applied to the front side of the solar cell, which results in an increase in the efficiency of the solar cell. A greater number of photons are able to reach the semiconductor materials as a result of this coating's ability to reduce light reflection. Light would be reflected by a solar cell that did not have an anti-reflection layer, rather than electrons being excited.

1.5 Types of Solar Cells:

There are different classifications for solar cells, including

- First Generation
- Second Generation
- Third Generation

The First-generation cells, also referred to as traditional or substrate-based cells, consist of solid silicon crystals. This PV technology, featuring materials such as polysilicon and single-crystalline silicon, is extensively utilized in the business world.

Second-generation solar panels are composed of thin-film technology, including amorphous silicon, CdTe, and CIGS cells. These panels hold significant economic potential for large-scale photovoltaic projects, integrating solar energy into buildings, and in compact, off-grid power solutions.

The third generation of solar cells encompasses several thin-film technologies that are seen as potential breakthroughs in solar energy. However, these technologies are still being explored or developed and have yet to gain broad commercial application.

Different types of solar panels can be classified into several groups.

1.5.1 Amorphous Silicon Solar Cell (A-Si)

Amorphous silicon PV modules were pioneers in the world of solar cells, being some of the earliest ones manufactured on an industrial scale. With the use of low processing temperatures, the manufacturing of a-Si solar cells becomes more cost-effective as it allows for the utilization of affordable materials such as polymer and other flexible substrates. These substrates require less energy to manufacture, which contributes to the overall energy efficiency of the production process flexible, other substrates are also available [23]. The non-crystalline and chaotic structure of amorphous silicon is what distinguishes it from monocrystalline silicon. Amorphous silicon has a substantially higher light absorption rate, roughly forty times faster than monocrystalline silicon. Due to their superior efficiency, amorphous silicon-based solar cells have gained more popularity compared to alternative materials like CIS/CIGS and CdSa/CdTe [24]. Deposition of amorphous silicon may also take place at extremely low temperatures, as low as 75 degrees Celsius, which enables the material to be placed on plastic without any problems. On the other hand, when single-layer cells are exposed to sunlight, they experience a significant reduction in their power output, which can range anywhere from 15 to 35 percent [25].

1.5.2 Biohybrid Solar Cell

Inorganic matter and organic matter are both components of a biohybrid solar cell, which is a type of solar cell that is created by combining the two types of materials. By using the photosystem, a photoactive protein complex located in the thylakoid membrane, the group managed to replicate the natural photosynthesis process, thereby increasing the efficiency in transforming solar energy [26]. A photosystem composed of many layers in order to generate a

current that travels through the cell, I first collect photonic energy, then transform it into chemical energy, and last gather it. Following a period of several days, the photosystem I become apparent and takes the form of a thin green coating. In order to facilitate and enhance the process of energy conversion, this thin film is helpful [27].

1.5.3 Buried Contact Solar Cell

A metallic contact is inserted into a cut-out groove created by a laser in a solar cell buried under the ground, a widely used solar technology praised for its superior performance. The buried contact method is able to overcome a significant number of the drawbacks that are associated with screen-printed contacts. Consequently, the efficiency of solar cells placed under the ground can surpass that of commercially printed solar cells by up to 25 percent. In a silicon-based solar cell, the metal layer is placed inside a trough cut by a laser, a key element that aids in the cell's high performance. This approach allows for a significant ratio between the metal's height and width. Consequently, this narrow trench enables the incorporation of a lot of metal into the contact finger, without the need for a broad metal layer on the outer face. This is because the metal contact aspect ratio is large [25].

1.5.4 Cadmium Telluride Solar Cell (CdTe)

Cadmium telluride photovoltaics, also referred to as CdTe photovoltaics, is a kind of photovoltaic (PV) technology that relies on a thin semiconductor layer called cadmium telluride. This layer is designed to capture and transform sunlight into electrical energy. Among various sizes, CdTe photovoltaics are the sole thin film technology for larger systems to offer cheaper prices than conventional solar cells constructed with crystalline silicon. For systems of more than one thousand kilowatts, CdTe photovoltaics remains the sole affordable thin film technology compared to crystalline silicon solar cells [28], [29]. CdTe photovoltaics boast the smallest environmental impact, the least water consumption, and the quickest return on investment in their lifetime when considering the overall lifecycle of these technologies. With a payback period of less than a year, it becomes feasible to achieve quicker reductions in carbon emissions without facing immediate energy shortages. Environmental concerns regarding the toxicity of cadmium can be alleviated through the recycling of CdTe modules once they have reached the end of their useful lives [30].

Cadmium is classified as one of the six most lethal and hazardous substances. Nevertheless, CdTe seems to possess a lower level of toxicity compared to pure cadmium, particularly when considering immediate exposure. However, it should be noted that it is not without potential damage. Cadmium telluride is poisonous when swallowed, breathed as dust, or mishandled.

1.5.5 Concentrated PV Cell (CVP and HCVP)

Heading towards the sun. A Concentrating Photovoltaic (CPV) system employs a sophisticated optical setup to focus a broad spectrum of sunlight onto each module, effectively transforming light energy into electrical power with exceptional efficiency, similar to the conventional photovoltaic approach. Concentrator photovoltaic (CPV) technology is a solar apparatus that transforms sunlight into electrical energy. This approach differs from standard photovoltaic setups by using lenses and curved mirrors to focus sunlight onto tiny yet highly effective multi-junction (MJ) solar cells [31]. Back in the 1970s, CPV technology was first introduced. Lately, advancements in this technology have enabled CPV to reach a point of economic feasibility and stand up against traditional fossil fuel power plants, such as those that operate on coal, natural gas, and oil, in areas where the climate is both sunny and arid. In the near future, highly concentrated photovoltaic (HCPV) systems are expected to become competitive. They boast the highest efficiency among all the currently available solar technologies, and the need for a smaller photovoltaic array also reduces the overall cost of the system. Currently, CPV is not utilized in the PV rooftop sector and is far less prevalent compared to traditional PV systems [32].

1.5.6 Copper Indium Gallium Selenide Solar Cells (CIGS):

The acronym CIGS stands for copper, indium, gallium, and selenide, and it is one of the most intriguing and divisive solar materials. Solyndra, NanoSolar, and MiaSolé were among the CIGS businesses that nearly became household names during this solar thin-film hype cycle. A copper indium gallium selenide (CIGS) solar panel is a form of thin-film photovoltaic panel designed to transform solar energy into electrical energy. This process entails depositing a thin layer of copper, indium, gallium, and selenide onto a glass or plastic base. Furthermore, metal strips are mounted on both the front and back of the panel to collect electrical charges. In contrast to various semiconductor materials, the compound in focus requires a much thinner coating due to its high light-absorption capacity and its strong capability to absorb sunlight [33].

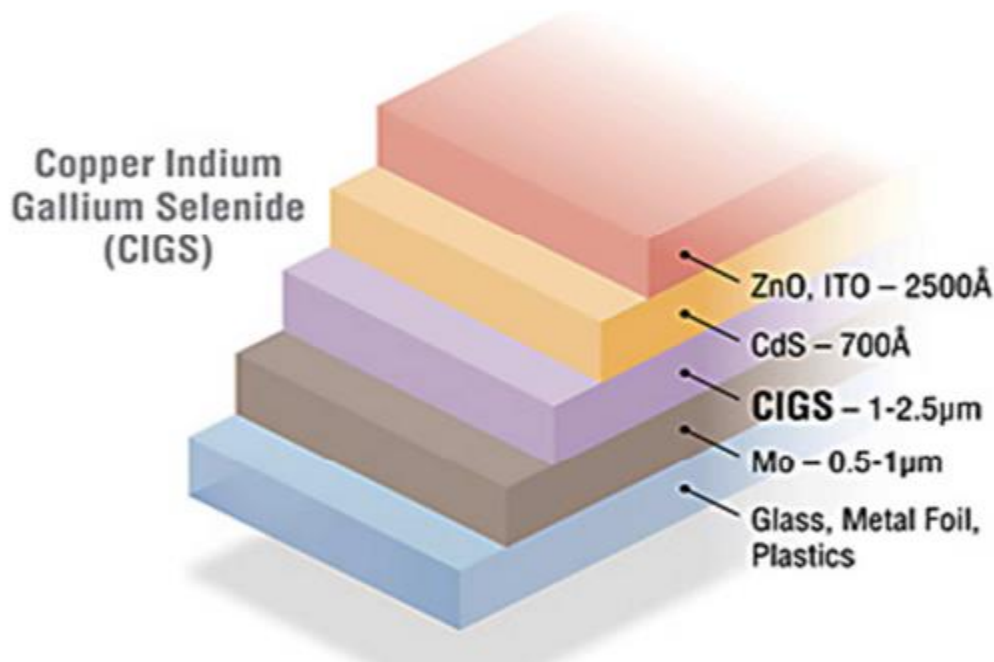


Figure 1-3 Graphic showing the five layers that comprise CIGS solar cells [32]

1.5.7 Dye-Sensitized Solar Cell (DSSC)

Dye-sensitized solar cells (DSSC), also known as dye-sensitized cells (DSC), represent the third generation of photovoltaic (solar) technology, capable of converting all visible light into electrical power. This advanced form of solar technology closely resembles artificial photosynthesis due to its ability to mimic nature's way of capturing light energy. The concept of dye-sensitized solar cells was first introduced by Professors Michael Graetzel and Brian O'Regan at the École Polytechnique Fédérale de Lausanne (EPFL) in Switzerland in 1991. They are often recognized as the Graetzel cells, but for the purpose of this discussion, we will use the term G Cell. DSSC, or Dye-Sensitized Solar Cells, stands out as a cutting-edge technology that can produce electricity under various indoor and outdoor lighting conditions, enabling users to convert both natural and artificial light into usable energy to power a range of electronic devices. Among the various thin film solar cell technologies, one cost-effective option is the dye-sensitized solar cell, also referred to as DSSC, DSC, or DYSC [34].

1.5.8 Gallium Arsenide Germanium Solar Cell (GaAs)

The chemical compound gallium arsenide consists of the base elements gallium and arsenic. The aforementioned chemical, which is formed when these two elements join together, exhibits

numerous intriguing properties. The semiconductor gallium arsenide outperforms silicon in terms of both saturated electron velocity and electron mobility. A semiconductor is a substance that displays conductivity that lies somewhere in between an insulator and a conductor in terms of electricity. This level of conductivity can fluctuate with changes in temperature, making it extremely useful across many uses. Gallium arsenide is a flexible material used in numerous gadgets, such as microwave frequency integrated circuits, integrated circuits that operate at the microwave frequency, light-emitting diodes that emit infrared light, lasers, solar panels, and materials for optical windows [35].

1.5.9 Hybrid Solar Cell

Combined solar cells merge the superior attributes of both natural and synthetic semiconductors. These dual-purpose photovoltaic systems make use of natural substances along with polymers that are capable of absorbing light effectively and moving electrons. The design incorporates synthetic materials for accepting and moving electrons in these dual-purpose cells. These photovoltaic systems stand out for their ability to be manufactured affordably through a process that can roll out the material at a large scale [36]. The active layer in these solar cells is created by blending an organic substance with another that has high conductivity for electrons [37]. These two substances are joined together at a junction to form a specialized active layer, which results in greater efficiency in converting sunlight into electricity compared to using just one of these materials. One material absorbs the light and transfers the created exciton, while another helps in breaking down the exciton. The charge is then separated when the exciton is made from the donor, and it becomes spread out across the donor-acceptor complex. The energy required to separate the exciton comes from the difference in energy levels between the highest energy electrons in the donor and the acceptor's highest energy levels [38]. After the exciton is broken down, the electrons move through a well-developed network of pathways to the electrodes. The exciton diffusion length is the average distance that an exciton can travel through a material before it is annihilated by recombination.

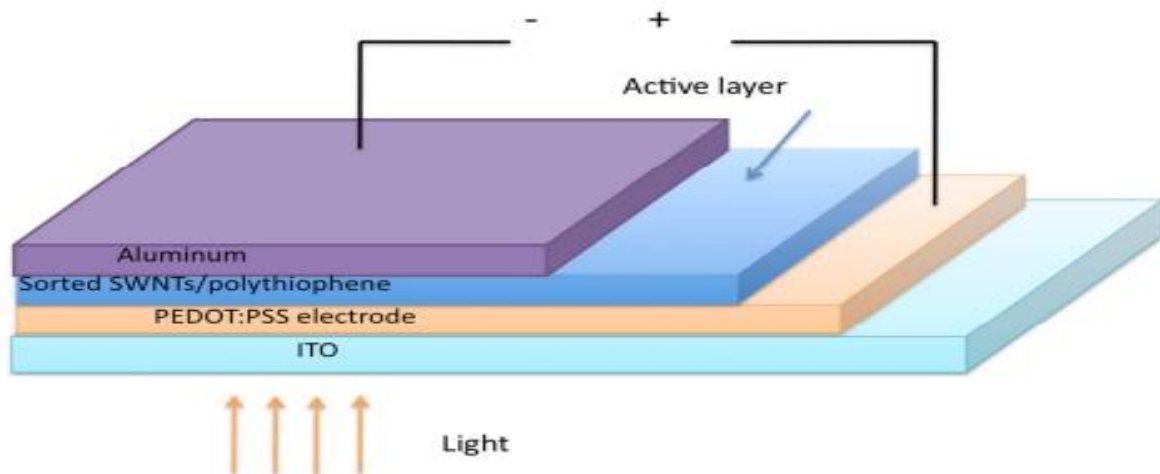


Figure 1-4 Structure of carbon nanotubes based solar cells [32]

1.5.10 Luminescent Solar Concentrator Cell (LSC)

A luminous solar concentrator (LSC) is a tool that uses a thin film to absorb solar light over a broad area, and then directs this energy through luminescent emission to cells at the narrow ends of the film. The thin film is often made of a polymer like polymethylmethacrylate (PMMA), which is packed with luminescent materials such as organic dyes, quantum dots, or rare earth compounds [39]. The main purpose of using LSCs is to replace an expensive array of solar panels in a conventional flat-plate PV panel with a more affordable solution. As a result, the cost of the module (£/W) decreases, along with the solar energy produced (£/kWh). A significant advantage of LSCs is their capability to collect both direct and scattered solar light, distinguishing them from standard concentrating systems. Thus, there is no need for sun tracking [40].

1.6 Why Organic Materials?:

The field of inorganic solar cell technology experienced a substantial advancement in 1954 when Bell Laboratories introduced the initial silicon cell [41]. Considerable advancements in the discipline have enabled the improvement of silicon solar cells, leading to the achievement of power conversion efficiency (PCE) levels as high as 25% [42]. Currently, silicon-based solar cells are utilized in the majority of photovoltaic systems that are implemented. The investigation of additional inorganic photovoltaic systems has yielded encouraging outcomes. Sharp Monolith has developed a 35% efficient inorganic solar cell utilizing GaInP [43].

OPVs and other emerging solar technologies may fill in holes in inorganic PV. There are numerous benefits to utilizing scalable roll-to-roll manufacturing techniques on flexible substrates. The expense is relatively diminished, and the scope of potential uses is more comprehensive.

Over the past two decades, organic photovoltaics (OPVs) have received significant attention due to their numerous advantages over inorganic solar cells [44]. Upon comparing inorganic and organic photovoltaic cells (PVs), it becomes evident that OPVs possess the following benefits: reduced weight, enhanced cost-effectiveness, and non-toxic characteristics. Flexible and mechanically robust as well. Roll-to-roll production at a low cost and on a large scale enables rapid commercialization. Nevertheless, organic solar cells exhibit a significantly diminished

power conversion efficiency in comparison to their inorganic counterparts. The maximal efficiency of OPVs is currently 13% at the moment [45]. OPVs face a challenge in terms of stability, as their present lifespan is restricted to 5000 hours, whereas silicon solar cells can endure for up to 20 years [44]. As a consequence of this, the most important objectives in OPV research are about enhancing the efficiency of power conversion and the stability of the system.

1.7 Varieties of Organic Solar Cell Device Structures:

The conventional configuration of organic solar cells comprises three distinct layer types: anode, cathode, and active. In the medium between the anode and cathode is the active layer. To promote efficient charge, transfer within the cell, it is necessary for one of the electrodes to possess light transparency. Indium tin oxide is frequently employed as a transparent anode layer, whereas the cathode layer is composed of a metal electrode such as calcium or aluminum. Considerable investigation has been undertaken regarding various device topologies for organic solar to improve the efficiency of charge transfer throughout the cell [46].

1.7.1 Organic single-layer solar cell

An organic photovoltaic device, a single layer organic solar cell consists of a photoactive material layer positioned between the anode and cathode layers [47]. Charge generation is enhanced through the combination of conjugated polymers with acceptor materials present in the photoactive layer. The cathode layer, which is commonly composed of a metal electrode, accumulates negative charges (electrons), while the anode layer, which is frequently composed of indium tin oxide, allows light to pass through while collecting positive charges (holes). This architecture makes it easier to make devices, but it might be hard to get good power conversion efficiencies with it. Photocurrent generation in single layer organic solar cell architectures is dependent on the work function difference that exists between an electrode and a metal electrode. Nevertheless, the effectiveness of this design in separating charge carriers is constrained, leading to a significant occurrence of hole-electron recombination [48]. Consequently, these architectural designs experience diminished efficacy. Merely 0.1% is the utmost power conversion efficiency attained through the utilization of this device architecture [47].

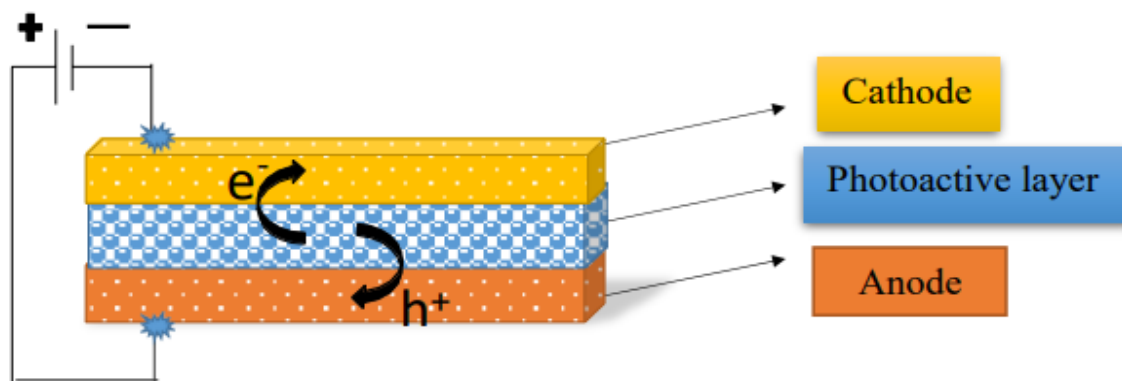


Figure 1-5 Organic Single-layer Solar Cell [49]

1.7.2 Organic Double Layer Solar Cell

A double-layer organic solar cell consists of two distinct layers of photoactive components and is classified as an organic photovoltaic device. The structure comprises a donor layer responsible for light absorption and excitation generation, and an acceptor layer designed to effectively partition the excitons into free charges. In general, the architecture of double-layer organic solar cells comprises an n-type electron acceptor layer and a p-type electron donor layer. Tang introduced this architectural design in 1986, employing perylene derivatives as the acceptor layer and phthalocyanines as the donor layer. Charge carriers are generated within a double-layer organic solar cell through the interaction of light with the donor molecules. Upon the separation of the donor and acceptor molecules, the charge carriers undergo migration toward the electrodes possessing opposite charges. To facilitate this motion, the LUMO and HOMO levels of the donor and acceptor molecules must be aligned. It has been reported that the highest power conversion efficacy attained by this architecture is 1% [47].

1.7.3 Bulk heterojunction (BHJ) organic solar cell

The architecture of the bulk heterojunction (BHJ) organic solar cell is widely used in organic photovoltaic systems. Alan Heeger's 1995 proposal of the bulk heterojunction (BHJ) device architecture represents a significant advancement in the field of organic solar cells [50]. This architectural configuration positions the active layer, which is situated between the anode and cathode layers, within a network composed of acceptor and donor molecules. Increased charge

carrier generation occurs at the interface of the donor and acceptor molecules due to the BHJ structure's larger interfacial area. This facilitates charge transfer between the electrodes in an efficient manner. In BHJ solar cells, conductive polymers such as poly (3-hexyl thiophene) are commonly employed as donors, while fullerene derivatives are utilized as acceptors. Tandem and inverted BHJ solar cells are instances of modifications to this structure.

By integrating a metal cathode layer with a transparent anode layer (e.g., indium tin oxide), this architectural design enhances charge separation. The broad interfacial area of the BHJ structure facilitates charge collection and generation, thereby enhancing the performance of the device. The architecture of a BHJ solar cell achieves a peak efficiency of 8.94% [50].

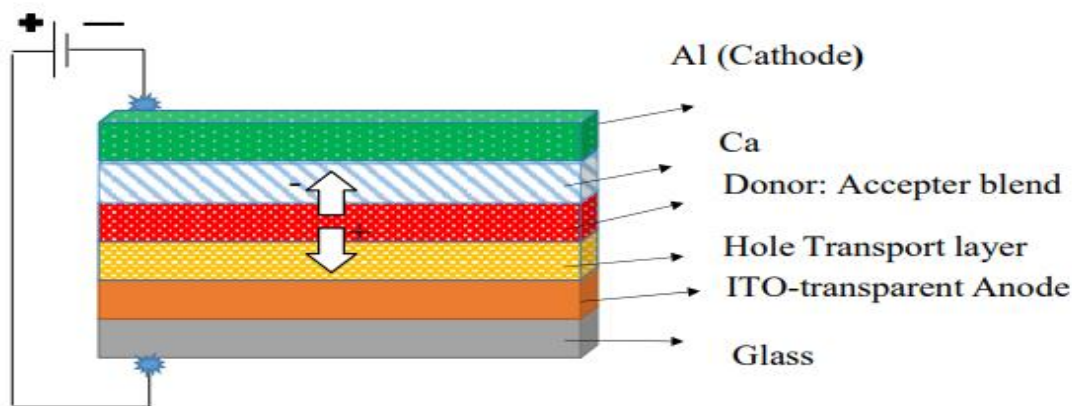


Figure 1-6 Bulk heterojunction (BHJ) [50]

1.8 Materials for organic photovoltaics (OPV):

A key component of an Organic Photovoltaic (OPV) cell is a thin film organic semiconductor (OS) material, which can be composed of polymers or oligomers. The active layer is situated between a transparent electrode and a metal electrode. Organic semiconductors commonly exhibit either electron-donating or electron-accepting properties [51]. Materials possessing the ability to donate electrons are referred to as electron-donor materials, while materials possessing the ability to accept electrons are known as electron-acceptor materials. The active layer in organic photovoltaic (OPV) systems has a blend of electron-donor and electron-acceptor components [52]. Fullerene functions as an electron-accepting material, while copper phthalocyanines (CuPc) act as an electron-donating substance. The active layer of OPV devices

comprises a mixture of organic semiconductor materials that function as both electron donors and acceptors [53].

1.8.1 *Electron-donor materials*

Electron-donor materials are substances capable of relinquishing or transferring electrons in chemical or physical reactions. Phthalocyanines and their derivatives are extensively researched organic semiconductors in the field of organic electronics. Their exceptional photophysical and electrochemical properties have resulted in their utilization as electron-donor or acceptor compounds in multicomponent systems for energy and charge transfer operations. Phthalocyanines are commonly employed as the primary components in these light-sensitive molecules due to their exceptional capacity to absorb light [54]. Copper phthalocyanines (CuPc) and zinc phthalocyanines (ZnPc) are metal-phthalocyanine compounds that find extensive application in organic photovoltaic (OPV) devices. Their primary function is to transport holes, while they function as prominent absorption materials when utilized as donors. Xue et al. conducted a study in which they obtained an efficiency of approximately 4% in a double-heterojunction thin film cell (CuPc/C60) using Ag as the metal cathode under four suns of simulated AM1.5G illumination. The ongoing research focused on (CuPc)/C60 cells featuring hybrid planar-mixed molecular heterojunctions has yielded a noteworthy increase in efficiency of 5.5% [55]. Significant interest has been generated in subphthalocyanines owing to their distinctive photophysical properties and chemical composition as the lowest homologs of phthalocyanines [56]. Greater energy level alignment and a larger open circuit voltage (V_{oc}) distinguish SubPc-based organic photovoltaic systems from those based on phthalocyanines, according to the findings of Kristin et al [57].

Consequently, the efficiency of the SubPc/C60 cell surpasses that of the CuPc/C60 cell. It has been demonstrated that porphyrins, their derivatives, and various oligomer organic substances are effective electron donors [58], [59]. However, one limitation of these devices is their restricted ability to function with flexible electronics. In photovoltaic cells, an assortment of polymer electron-donor materials have been effectively implemented as active layers. Among these, poly(3-alkylthiophene) (P3AT) has been utilized extensively as an active material.

P3HT is the most extensively utilized P3AT material in solar applications, with a 5% efficiency rating [60].

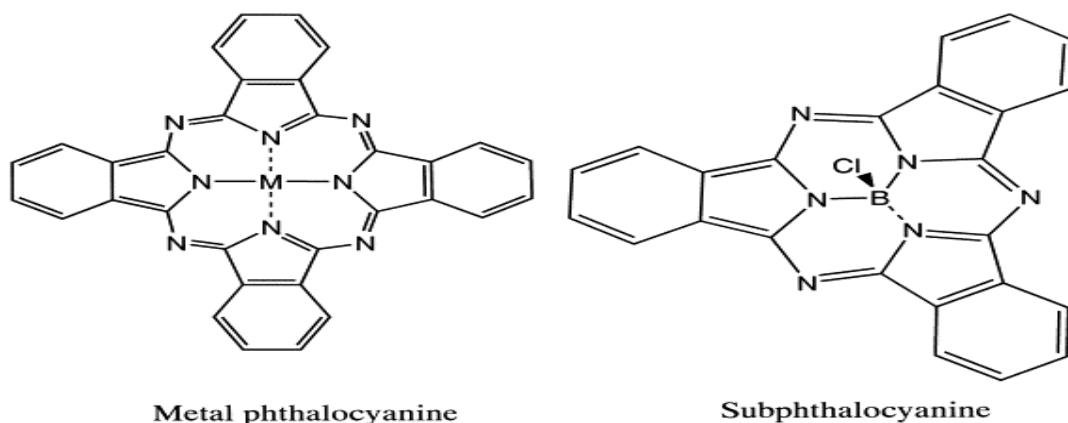


Figure 1-7 Examples of electron-donor materials [61]

1.8.2 *Electron-acceptor materials*

Throughout history, organic photovoltaic cells have implemented an extensive range of organic electron-acceptor materials. This has included conjugated polymers and minuscule molecular compounds. Nevertheless, only a limited number of these substances have exhibited the capacity to be utilized in high-efficiency OPV devices.

Fullerenes and their derivatives (see Figure 1.12), including C₆₀, are widely recognized and effective electron-acceptor materials. Notably, C₆₀ demonstrates remarkable molecular orbital arrangements and symmetry, which contribute to the emergence of captivating chemical and physical characteristics [62]. PC60BM and its derivative PC70BM have gained significant popularity as acceptors in OPVs in recent years on account of their advantageous solution process capability. PC70BM exhibits enhanced absorption in the visible spectrum when compared to PC60BM; however, its higher cost and lengthy purification procedure restrict its extensive implementation in optical photovoltaics [63].

Other than fullerenes, the derivative known as indene fullerene has been used as an electron acceptor material in organic photovoltaics (OPVs).

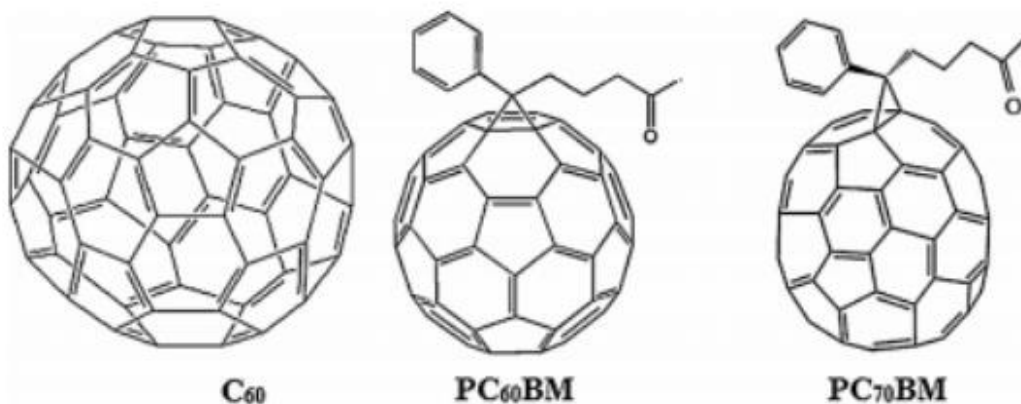


Figure 1-8 Examples of electron-acceptor materials [63]

1.8.3 Donor-acceptor polymer

Light absorption in organic photovoltaic (OPV) devices has conventionally been attributed to the donor material, as the majority of fullerene acceptors exhibit weak absorption in the visible and near-infrared regions, which coincide with the apex of solar radiation. As a result, a substantial amount of scholarly investigation has been devoted to the reduction of the polymer's optical bandgap (E_g). Donor-acceptor (D-A) hybridization, wherein the polymer backbone is adorned with alternating electron-rich and electron-poor segments, is presently prevalent in OPVs [64].

The hybridized molecular orbitals generated by the molecular orbital mingling between the conjugated donor (D) and acceptor (A) units have a smaller effective bandgap (E_g) than those of the constituent molecular orbitals. As a result of their capacity to generate significantly narrower bandgaps compared to backbone planarization alone, D-A polymers are gaining prevalence in OPV research [65].

1.8.4 Electron donor-acceptor-donor (D-A-D)

Organic solar cells possess the capacity to facilitate the creation of photovoltaic devices that are both economically viable and employ environmentally sustainable technology, thereby minimizing their ecological footprint. Soluble conjugated polymers continue to be a significant

class of materials employed as donors in organic photovoltaics (OPV) [66], [67]. There has been an increasing emphasis on small molecule donor materials in recent years. In contrast to polydisperse polymers, the well-defined chemical structure of these substances confers benefits in terms of reproducibility during synthesis, purification of the material, and performance of devices. It is also easier to analyze structure-property relationships when molecules are utilized, which is essential when developing efficient photovoltaic materials. As donor materials, symmetrical molecules with a donor-acceptor-donor (D-A-D) structure originating from various classes of active molecular materials have garnered the attention of scientists in recent years [68], [69], [70].

1.9 Computational Studies:

Molecular behavior and properties are analyzed by computational chemistry via simulations, algorithms, ab initio methodologies derived from quantum chemistry, and empirical techniques [71]. A variety of equations and algorithms are utilized in computational chemistry to solve chemical problems. Computational chemistry provides a reliable approach for forecasting the varied properties of molecules that are impracticable to ascertain through experimental means. Moreover, it assists experimental chemistry in the identification of the most effective methodology or mechanism.

The application of sophisticated computer programs in conjunction with theoretical chemistry techniques is utilized to compute the energies, molecular structures, and properties. The techniques employed in this context consist of ab initio, semi-empirical, molecular dynamics, molecular mechanics, and Density Functional Theory (DFT) methodologies [72].

Computed methods frequently rely on principles derived from both classical and quantum mechanics.

1.9.1 Classical Mechanical Methods

Classical mechanics-founded approaches frequently comprise the molecular dynamics method and the molecular mechanical approach. These techniques both employ Newton's law [73].

1.9.1.1 Molecular Dynamics (MD)

Molecular dynamics pertains to the application of computational simulations to examine the ever-changing characteristics of atoms and molecules. The trajectory of atoms and molecules is

determined within the field of Molecular Dynamics (MD) by implementing of the numerical solution to Newton's equation of motion. This equation characterizes the behavior of a system comprised of interacting particles, with the forces between these particles and their corresponding potential energies frequently calculated using molecular mechanics-based force fields or interactions between atoms [74].

1.9.2 Molecular Mechanics (MM)

Molecular mechanics is a subfield of classical mechanics that models the molecular system using the Born-Oppenheimer approximation. The force field determines the potential energies of all systems following their nuclear coordinates [75].

1.10 Quantum Mechanical Methods:

Quantum mechanical (QM) methodologies postulate that the nucleus exerts an influence on the electron motion within a molecule. Quantum mechanical (QM) processes predominantly involve the approximation of the Schrodinger equation solution, which aims to determine the atomic forces, electronic configuration, and energies of a given molecular system. In addition to chemical pathway information, these technologies also furnish thermodynamic data such as heat of production. Computational methods grounded in quantum mechanics consist of ab initio, semi-empirical, and DFT techniques [76].

1.10.1 Ab- initio method

By leveraging the wave function (ψ), the ab initio method is utilized to ascertain the energy of a molecule in accordance with the Schrodinger equation. The utilization of the wave function to determine the spatial arrangement of electrons enables the forecasting of a multitude of molecular characteristics. The ab initio method is distinguished from semi-empirical methods by its considerably greater computational time demand [71].

1.10.2 Semi-Empirical method

The semi-empirical methodology is predicated on Schrodinger equation principles. The methodology entails the integration of empirical data and theoretical principles, with the experimental findings serving as parameters for the Schrodinger equation. The semi-empirical approach exhibits greater time efficiency when compared to the ab-initio methodology [77].

1.10.3 Density functional theory (DFT) method

The utilization of density functional theory (DFT) techniques has proven to be exceptionally effective when examining molecular properties. Density functional theory (DFT) methodologies are predicated on the energy of a particle, as described by the Schrodinger equation. Within this particular framework, the energy is predicated upon the electron density, which is likewise determined by the spatial coordinates (x, y, z). The utilization of Density Functional Theory (DFT) extends to a diverse array of electronic characteristics, encompassing solvation behavior, potential energy surfaces, Hirschfield charge analyses, geometry optimization, infrared (IR), and nuclear magnetic resonance (NMR) investigations, among others. The hypothesis formulated by Kohn and Sham investigates the electron density and its link with the molecule energies in the provided equation [78].

$$\mathbf{E} = \mathbf{E}^V + \mathbf{E}^T + \mathbf{E}^J + \mathbf{E}^{\text{XC}}$$

The symbols \mathbf{E}^V signify potential energy.

\mathbf{E}^T signifies the notion of kinetic energy.

\mathbf{E}^J represents the energy resulting from the repulsion between electrons.

\mathbf{E}^{XC} denotes the energy associated with the interchange and correlation of electrons.

The DFT approach was further divided into two variants due to differing assumptions.

1.10.3.1 LDA (Local Density Approximation)

This approach is a major method of estimating the electron correlation energy in Density Functional Theory (DFT), which is based on evaluating the electron density at each spatial coordinate. The precision of this estimation is contingent upon the presupposition of a uniform electron density within a certain molecule. The Local Density Approximation (LDA) estimation approach may not be suitable for particles with non-uniform electron density in any situation [79].

1.10.3.2 Gradient Generalized Approximation

The GGA method is an extension of the LDA strategy that is specifically designed to handle non-uniform estimations of electron density. The GGA correlation energy technique is highly appropriate for studying intermolecular interactions that include two or more molecules.

CHAPTER 2: LITERATURE REVIEW

This chapter will examine the notable progress and important observations on the use of organic materials in solar cells. The capacity of organic photovoltaics (OPVs) to fundamentally transform the landscape of renewable energy generation has attracted much attention in recent years. This article will analyze the fundamental concepts underlying organic materials in solar cells, along with their latest progress, challenges, and prospective future uses. We will examine the fundamental principles of organic photovoltaics (OPVs), discuss the many organic materials utilized in their production, analyze the latest research findings, and emphasize the advantageous environmental and economic impacts of this pioneering technology. The objective of this review is to provide a comprehensive examination of the present state of organic materials in solar cells and to shed light on their potential for widespread utilization in the generation of renewable energy.

2.1 Historical background of Photovoltaics:

Becquerel produced a noteworthy breakthrough by uncovering the photovoltaic effect around 1839. This event took place when platinum electrodes, which were coated with silver halogen, were subjected to illumination within a solution of water. The phenomenon is commonly known as the photo-electrochemical effect [80]. During the time frame of 1875-1880, William Adams and Richard Day discovered a comparable result with selenium when it was placed between two metallic electrodes, thereby creating the first solid-state photovoltaic device [81]. The functionality of this gadget relied on the utilization of metal and selenium to achieve the photovoltaic effect. Charles Frits made a significant contribution to the advancement of the discipline by inventing the first photovoltaic device with a wide surface area in 1883. The initial cells were equipped with a metal electrode, a semiconductor, and a thin, partially transparent metal electrode featuring a bottle neck design that facilitated the transmission of incident light. However, because to the limited design, the power conversion efficiency was less than 1% [82]. In the 1970s, the worldwide oil crisis prompted a surge in research and development in photovoltaic (PV) technology, resulting in substantial enhancements in the performance of PV cells. The research focused on the progress of device physics and process technology [83].

Extensive research was conducted on methods to reduce the manufacturing expenses associated with thin film technologies that rely on amorphous or microcrystalline silicon. Researchers conducted studies on tandem cell topologies and the manipulation of semiconductor materials' band gap to improve power conversion efficiency. The user's text is empty. Nevertheless, the improvement in mass production of infrared for semi-conducting devices was still insufficient, resulting in excessive production costs compared to those of oil.

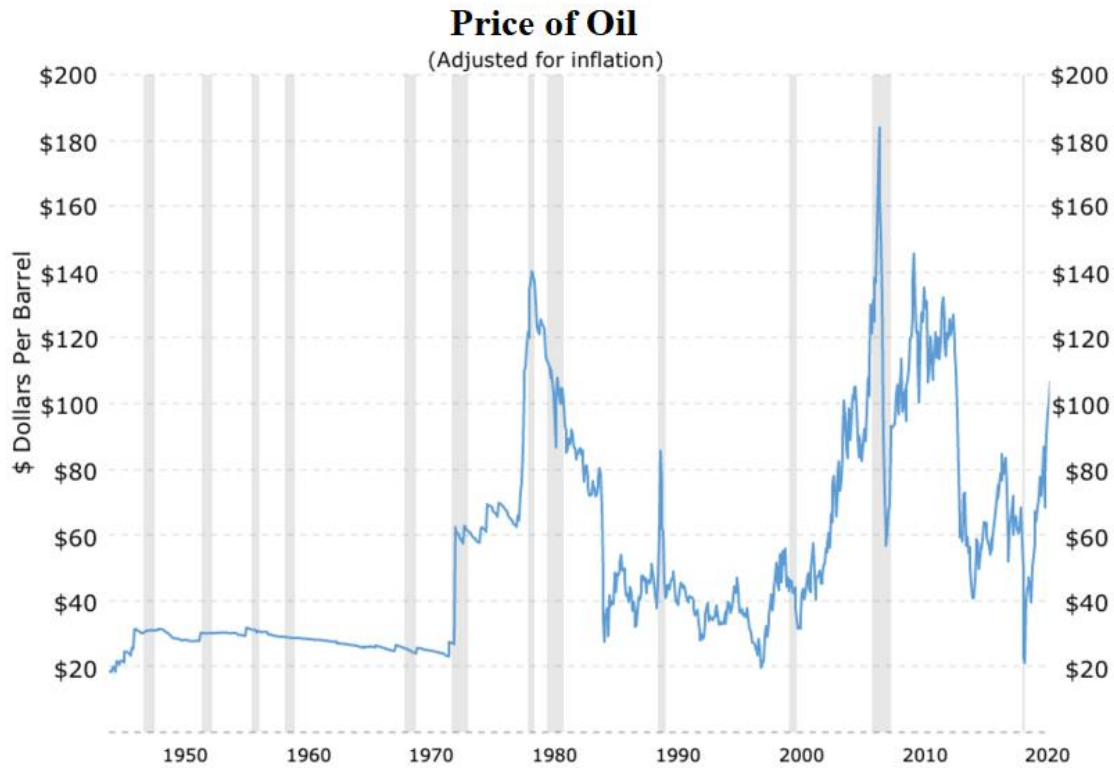


Figure 0-1 Oil Crisis [84]

In the 1990s and 2000s, interest in photovoltaics increased significantly. Several factors contribute to this heightened emphasis, including the deregulation of energy and mounting concerns regarding environmental issues like climate change. These concerns have significantly influenced the strong motivation to explore and acquire alternative energy sources [85].

Given the recent surge in oil prices, which have soared to approximately \$150.00 per barrel, governments and businesses alike have been compelled to explore alternative energy sources as a means of diminishing their dependence on oil. In many countries, governments offer discounts on a significant portion of the installation costs for PV systems. This has greatly accelerated the

growth of businesses that rely on PV technology. In the early 1900s, PV technology began making a significant impact on the world by encouraging the transition from fossil fuels to renewable energy sources [86].

Photovoltaics are becoming more popular as an option to fossil fuels because they are cheap to set up, work very well, and can be used in any way in the future [87]. Monocrystalline silicon, polycrystalline silicon, amorphous silicon, cadmium telluride, copper indium gallium diselenide, and copper indium gallium diselenide are among the materials currently utilized in the construction of solar cells. Over the past several years, there has been a significant enhancement in the efficiency of solar energy systems. Although silicon cells exhibit a remarkably high level of efficiency, their utilization is limited by the inflexibility of their architectures and the protracted duration needed for cost and electricity payback. Emerging solar technologies such as Organic Photovoltaics (OPVs) have the potential to address deficiencies in traditional inorganic photovoltaic systems. The implementation of scalable roll-to-roll manufacturing processes on flexible substrates renders them particularly advantageous. This approach significantly lowers costs while broadening the spectrum of applications.

2.2 Organic Photovoltaic Cells:

Research on organic solar cells has advanced over the last three decades, but in the last decade in particular, a significant increase in power conversion efficiencies has sparked scientific and economic interest. Through the introduction of novel materials, the advancement of materials engineering, and the development of more intricate device structures, this achievement has been realized. Solar power conversion efficiencies exceeding 3% have been attained to date, primarily through the adoption of various device concepts. However, it must be noted that these efficiencies do not approach those achieved with inorganic solar cells. Nevertheless, the realm of organic solar cells has experienced significant advantages in recent times due to the entry of light-emitting diodes (LEDs) into the market, which utilize similar technologies. In this article, we will explore the current status of organic solar cells, discuss a variety of production technologies, and analyze the critical parameters that enhance performance [88].

2.3 Organic Materials in PV Cells:

The exploration of designing materials that exhibit activity through the manipulation of precisely defined molecules is becoming an area of interest in the pursuit of creating organic photovoltaic cells (OPV) that are both economical and ecologically sustainable. When compared to polydisperse conjugated polymers, synthesis and purification consistency are enhanced by molecular donors that are precisely defined. Greater control over the composition of materials and the efficacy of devices. Moreover, molecules support a more precise analysis of the connections between structure and properties, which advances material design [89].

2.3.1 Donor Materials

A multitude of molecular donor materials have been synthesized and subjected to evaluation in the recent years, with the aim of identifying potential donor substances for use in vacuum-deposited, solution-processed, and organic photovoltaic (OPV) cells.

2.3.1.1 Phthalocyanines

Phthalocyanines are frequently utilized as donor units within photoactive molecules owing to their unparalleled ability to absorb light. Using the bulk heterojunction design and phthalocyanine derivative C6PcH₂, organic thin-film solar cells have demonstrated exceptional performance metrics. The structure of the cells consists of a C6PcH₂: PCBM/Al indium–tin–oxide/polymer hole transport layer. They possess an external quantum efficiency surpassing 70% within the Q-band absorption region, coupled with an energy conversion efficiency of 3.1% [90].

2.3.1.2 Tin (II) phthalocyanines

Analyzing the effect of SnPc thickness on the electrical properties of organic solar cells (OSC) utilizing tin (II) phthalocyanines (SnPc)/C60 heterojunction, the study evaluated the performance of OSC. The findings indicated a power conversion efficiency of 0.79% under 1.5G solar illumination [91].

2.3.1.3 Metal phthalocyanines

Metal phthalocyanines (m-Pc) are superior to conventional phthalocyanines (CuPc, ZnPc) as donors in organic solar cells (OSCs). By altering the ratio of donors to acceptors for distinct m-Pc donors, Schottky OSCs with a high acceptor content can achieve improved performance. The

near-infrared absorption potential of Chloroindium phthalocyanines (ClInPc):C60 OSCs indicates the possibility of exceeding 1V at high efficiencies and voltages. Since the J_{sc} is dependent on the equilibrium between m-Pc Q band and C60 aggregate absorption, the research demonstrates that ClInPc is an appropriate donor for semi-transparent OSCs. m-Pcs' straightforward synthesis and purification could result in inexpensive and effective organic photovoltaics [92].

2.3.1.4 Copper phthalocyanines

The donor–acceptor bilayer solar cells of small-molecular-weight organic double hetero junctions are influenced by the purity of copper phthalocyanines (CuPc). Under AM1.5G, one sun illumination, improved CuPc purity enhances the power conversion efficiency from $0.26 \pm 0.01\%$ to $1.4 \pm 0.1\%$. The hole mobility of unpurified CuPc is approximately three orders of magnitude lower than that of pure material. Principally contaminating is metal-free phthalocyanines, which diminishes device performance and hole mobility [93]. By serving as a buffer layer in organic solar cells (OSCs), copper phthalocyanines nanoparticles (CuPc-NPs) improve photovoltaic parameters. V_{oc} 0.24 to 2.57 (mean 1.29), a fill factor of 0.465, and a power conversion efficiency of 5.22% were all achieved by the optimized OSC, which was attributed to enhanced interface characteristics and effective charge transfer [94].

2.3.1.5 Sub-phthalocyanines

In OPV, SubPc is frequently employed as an electron-donor material on account of its exceptional energy-level alignment. Tc: SubPc OPV devices utilizing tetracene (TC) as an electron donor and SubPc as an electron acceptor recently demonstrated 2.9% efficiency, according to research by Beaumont et al [95].

Organic solar cell (OSC) efficacy is enhanced through interface engineering, which optimizes charge transfer, collection, and recombination. By employing non-conjugated tetrasodium iminodisuccinate (IDS) as an electron transport layer, conventional PTB7-Th: PC71BM OSCs increase power conversion efficiency to 9.45% [96].

2.3.2 *Acceptor Materials*

BHJ devices require an electron acceptor alongside to the light-absorbing polymer donor for effective operation. Materials that have been utilized for this objective since the inception of OPV research have almost exclusively consisted of fullerene and fullerene variants.

2.3.2.1 Fullerene (C60)

A thin buffer layer is necessary for an organic solar cell employing fullerene (C60) as the acceptor to order to attain a significant power conversion efficiency. According to the scientists, the buffer layer in organic solar cells facilitates free carrier collection with a favorable electric field by impeding electron transmission from the metal to C60. This hypothesis was validated by the transient photovoltaic method, indicating that the buffer layer does not account for the exciton-blocking effect [97]. For organic photovoltaic cells, mixed films of boron subphthalocyanines chloride (SubPc) and C60 are evaluated. These cells operate most efficiently at 78% C60, but the SubPc-to-C60 ratio has a significant impact on output. This blend enhances the structural pattern of the active layer, thereby increasing hole mobility. With the better SubPc:C60 ratio, organic photovoltaic cells can turn virtual solar light into electricity with a 3.7 ± 0.1 % efficiency [98]. The use of solution-processed mixes in the creation of photovoltaic cells, with anthradithiophene derivatives acting as donors and fullerene derivatives acting as acceptors. Solvent vapor annealing makes spherulites, which have a direct effect on how well the material works. A good cell alongside 82% spherulites coverage got a 1% power conversion efficiency, showing that solution-processed tiny-molecule photovoltaic cells have a lot of promise.

2.3.2.2 Fullerene derivatives

Polymer solar cells, or PSCs, are used to change light between electrodes. They are made up of mixed polymers and liquid fullerene acceptors. A lot of people use PC60BM and PC70BM, but new developments in fullerene substitutes have led to the creation of other materials that are better in many ways.

2.3.2.2.1 PC60BM and PC70BM

Researchers looked at two different types of electron acceptors (PC60BM and PC70BM) in P3HT-based polymer solar cells (PSCs). Strong visual absorption in PC70BM-based cells made them work better. PC60BM cells were absorbing less. Because PC70BM molecules are bigger,

they can absorb more photons and move charges around more easily. Performance is changed by the absorption of photons, exciton dissociation, and charge transfer [99].

2.3.2.2.2 Indene-C70 Bisadduct

The commonly used receiver material PC60BM isn't great for polymer solar cells because it doesn't absorb light well and doesn't have a lot of energy. This is why a new soluble C70 derivative with a higher LUMO energy level was created. It is called indene-C70 Bisadduct (IC70BA). IC70BA works better than P3HT-based PSCs because it has a greater voltage and greater power transfer efficiency. This could mean that efficient PSCs don't need to be used anymore [100]. When 3 vol% of MT or HT are added as processing aids, polymer solar cells with P3HT as the donor and IC70BA as an acceptor work better as photovoltaic devices. X-ray diffraction, atomic force microscopy, and UV-vis absorption spectroscopy all show that the absorbance, crystal structure, and film form have all changed. Without additives, the conversion of power efficiency (PCE) goes up from 5.80% to 6.69%.

2.3.3 Donor-Acceptor materials

Due to fullerene acceptors aren't very strong in the visual and near-IR ranges, the donor is usually the one that absorbs light in OPV devices when the sun is shining the brightest. This means that a lot of studies have made the visible band gap E_g of polymer smaller. The bandgap in semiconducting polymers is caused by π -orbital overlap. This can be lowered by making the polymer backbone more flat, which makes conjugation last longer.

There are several different ways that chemists have tried to lower the optical bandgap of polymers. They have also made the quinoidal character stronger and reduced twisting along the backbone of the polymer. In the past ten years, (Donor-Acceptor) polymers containing the benzo[1,2-b:4,5-b] dithiophene (BDT) unit have had a lot of success. Single junction and tandem devices have around 9-10% efficiencies [101], [102].

2.3.3.1.1 Benzodithiophene (BDT)

The benzodithiophene (BDT) unit, which has a lot of electrons, works well with linked polymers. The material's symmetrical and coplanar shape makes it easy for charges to move through π - π interactions between molecules. For organic field-effect transistors, benzodithiophene (BDT) polymers were created and made. The amazing hole motion measured

in 0.25 cm²/Vs in these polymers is truly amazing [103]. In 2008, Yang and his colleagues created BDT-based donor-acceptor-linked polymers for use in organic photovoltaics (OPVs) [104]. The TT unit is a special thiophene-based building block that is used to make p-type conjugated polymers. It can change its shape to a quinoidal resonance pattern along the conjugated backbone, which lowers the energy of the bandgap [105]. The latest photoactive donor for organic photovoltaic cells (OSCs) is a donor-acceptor-linked polymer based on benzodithiophene (P1). It is easy for halogen-containing and non-halogen-containing organic solvents to be able to dissolve P1. It also has a large absorption curve. Chlorobenzene polymer had a PCE of 2.8%, but diphenyl ether increased it to 5.2%. This shows that the polymer could make things work better, creating a new group of high-performance OSC polymers that don't react with air [106].

2.3.3.1.2 Coplanar tricyclic dithiophene (CPDT)

Tricyclic coplanar dithiophene materials can be used to make organic molecules that can be used in several optoelectronic uses. The structural and molecular characteristics of these entities can be altered by modifying the bridging atoms. Carbon-bridged 4H-cyclopenta[2,1-b:3,4-b'] dithiophene, or CPDT, was initially necessary for the synthesis of donor-acceptor linked polymers, particularly for polymer solar cells (PSCs) [107]. The addition of two alkyl groups to the carbon bridge of CPDT enhances the solubility of the resulting copolymer. Poly[2,6-(4,4-bis(2-ethylhexyl)-4H-cyclopenta[2,1-b:3,4-b'] dithiophene)-alt-4,7-(2,1,3-benzothiadiazole)] was synthesized by Zhu and his colleagues. (P1), a solid-state thin film possessing a 760 nm absorption peak and demonstrated significant intermolecular interactions between chains. In 2007, P1 and PC71BM worked together to get a 3.5% power conversion efficiency [108].

2.3.3.1.3 Naphthodithiophene (NDT3)

Naphthodithiophene (NDT3) is the source of a new group of semiconducting polymers that have been studied for their big system and donor-acceptor framework, which helps them stack tightly. PNDT3NTz-DT is a stretchy polymer that can convert 5% of its weight in electricity into heat and has a high field-effect mobility. This makes it an exciting core unit for semiconducting polymers and a hopeful design technique for high-performance polymers [109].

2.3.4 Donor-Acceptor-Donor

Organic photovoltaic cells make it possible for solar devices to be made that are both cheap and good for the environment. Soluble polymers with conjugation are still the most common donor compounds for OPV, but small molecule-based materials have become more popular in recent years. Molecules have better consistency, purity, and device performance than polydisperse conjugated polymers because of their unique chemical structure. However, molecules make it easier and more reliable to study the links between structure and properties, which is why they are so important for designing materials that convert light into electricity [110]. Molecular materials characterized by conjugation and composed of symmetrical molecules featuring a D-A-D structure have recently attracted considerable attention due to their potential as sources for active molecules. Triphenylamine (TPA) is a very interesting choice over organic photovoltaic uses because it can quickly donate electrons and help holes move around [111]. A lot of study has been done on small molecules based on TPA that can be used in organic solar cells (OSCs). There are both star-shaped molecules with TPA in the middle and straight structures with TPA at the end of these small molecules [77].

Recently, a TPA-based straight D-A-D small molecule with a thiazolothiazole (TT) receptive unit was reported. It has PCE values as high as 3.7% [80]. Through Stille coupling, a new organic molecule (M1) was made that has an isoindigo electron acceptor and a triphenylamine electron donor. M1 takes in light between 300 and 700 nm, which has a relatively low HOMO level of energy, and holes move around a fair amount. Solar cells worked at 0.84% efficiency [112]. For organic solar cells that are built on solutions, two new molecules have been created: TPA-TV-PM and TPA-HTV-PM. These molecules, which are made up of triphenylamine, pyran, as well as thienylenevinylene, can absorb a lot of visible light and have lower HOMO energy levels. This means that solar cells can work at 2.06% to 2.10% efficiency under AM1.5 illuminations [113]. Two D-A-D systems were made, one with isoindigo as the acceptor and benzo furan as well as dithienopyrrole as the donors. The electrical characteristics of these systems were analyzed through cyclic voltammetry and UV-Vis absorption spectroscopy. The material's properties and performance of solar cells were greatly affected by the presence or lack of nitrogen substitution [114].

2.3.4.1 The photovoltaic mechanism behind A–D–A molecule based devices

In an organic photovoltaic technology, the photovoltaic process is made up of four main steps, which are: (1) photon absorption and exciton, (2) moving exciton around, (3) breaking up excitons and separating charges, and (4) moving and collecting charges.

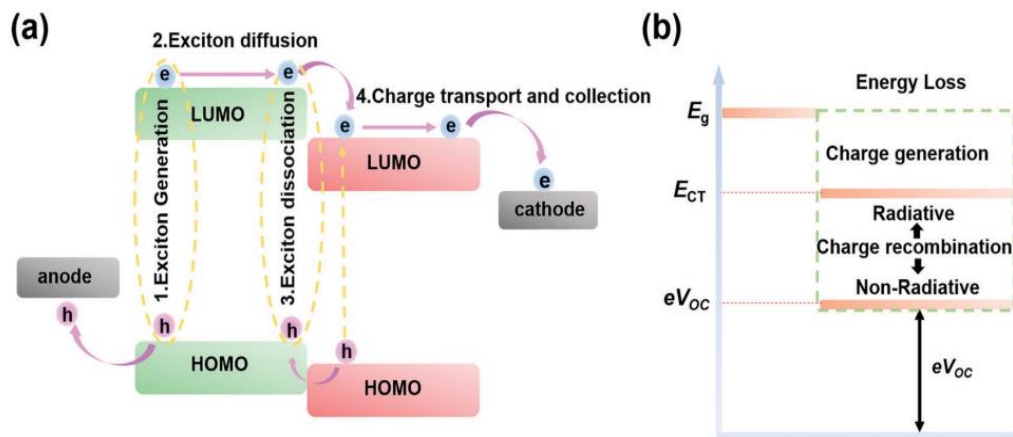


Figure 0-2 Working mechanism of OPVs [115]

The third step is very important because it determines the EQE (J_{sc}) and FF. It needs to be very efficient at separating exciton and charge with no charge recombination [67]. In the third step, the link between donor and recipient molecules in the active layer is very important, if not perhaps the most important one. While both the acceptor and donor entities are excited, step 3 of exciton breakup and charge separation takes place. This means that the interaction should mostly rest on their LUMO orbitals and how they interact with each other [116].

2.3.5 Goals and Purposes:

The aim of this thesis is to utilize Density Functional Theory (DFT) to conduct a thorough examination of the electronic and structural characteristics of Fullerene and Non-Fullerene donor materials employed in Organic Photovoltaic (OPV) cells. It is widely recognized that the donor and acceptor units are the primary subject of investigation in organic photovoltaic cells. We conduct a comparative analysis between fullerene-based and non-fullerene-based donor materials to assess their respective advantages and limitations in OPV applications. Meanwhile by using insights gained from DFT simulations to propose and design novel donor materials with

enhanced photovoltaic properties. This may involve modifying molecular structures to improve charge transport, reduce energy losses etc. At the end by attaching methyl, ethyl and propyl groups with acceptor part of cell we also wanted to predict the behavior and study the variation in different photovoltaic properties of the cell.

CHAPTER 3: METHODOLOGY

The primary aim of this research was to utilize DFT computation to compare the different donor parts of organic photovoltaic cells in D-A-D structures. Following is the flow chart of computational study.

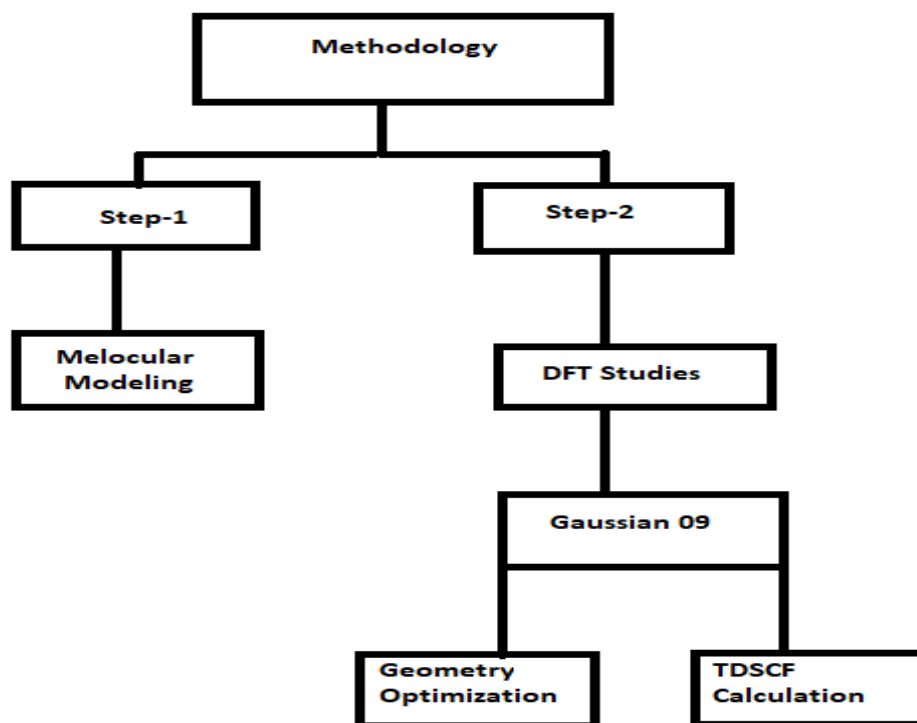


Figure 0-1 Methodology Flow chart of Computational Modelling

3.1 Molecular Modelling:

Molecular modelling is a scientific method that represents the spatial arrangement of molecules using the coordinates x , y , and z in three dimensions. Subsequently, these structures undergo geometry optimization to ensure adherence to key chemical laws and theories. The domain of molecular modelling is extensive and possesses significant potential. Over the last ten years, it has developed to include activities such as optimizing, predicting, simulating, and analyzing the behaviors of molecules in both real-time and passive time. This technique has significantly

transformed computational science, allowing for efficient resolutions to chemical issues and generating a novel field for progress [117].

Molecular modelling plays a crucial role in the progress and optimization of organic photovoltaics (OPV). Organic photovoltaics is a specialized study area focused on the development and manufacture of highly efficient solar cells using organic materials. Scientists can utilize computational tools to investigate and improve the efficiency of OPV systems.

The current study utilized molecular modelling to synthesize an organic compound. The inquiry specifically examined the effects of different donor parts as well as the increase of carbon chain of Acceptor part in D-A-D structures. The objective of this research endeavor was to improve understanding and support future progress in this specific area of study. The molecular geometries were modelled using the GUI Gauss-View06 and Gaussian 09 software.

3.1.1 GaussView06

GaussView06 is an extensively used graphical user interface which is frequently used with the Gaussian chemical computation software. The main objective of this software is to streamline the configuration of different Gaussian calculations by offering a user-friendly interface. The software provides sophisticated functionalities, including a molecule builder that enables the generation of three-dimensional chemical representations of molecular systems [118]. In addition, Gauss View 06 allows users to easily create and run Gaussian input files eliminating the requirement of manual programming instructions. In addition, it has advanced visualization capabilities, enabling graphic representation of Gaussian output files using features such as graphs, spectra, and animated vibration. In general, researchers in computational chemistry will find that using Gaussian is now easier and faster with Gauss View 06.

3.2 Gaussian-09:

John Pople and colleagues created the now-popular software program Gaussian-09 in 1970 under the codename Gaussian-70. It finds extensive use in the field of computational chemistry [119]. For a wide variety of computational chemistry and biochemistry activities, it is an invaluable tool for chemists, biochemists, chemical engineers, and material scientists. The software allows users to calculate molecule structures, characteristics, and reactions using multiple levels of theory,

including molecular mechanics (MM), ab initio, Semi Empirical, as well as Density Functional Theory (DFT). The incorporation of integrated standard basis sets, like STO-3G, 3-21G, 6-21G, 4-31G, 6-31G, 6-311G, LANL2DZ, SDD, and others, is a major benefit of Gaussian-09. By mathematically defining molecule orbitals, these basis sets allow efficient and precise quantum chemical calculations. With its extensive library of algorithms and basis sets, Gaussian-09 is a robust and flexible computational chemistry software program that can handle a broad variety of computational investigations in the chemical sciences [120].

3.3 Density functional theory (DFT):

The electronic structure and characteristics of atoms, molecules, and solids can be studied using density functional theory (DFT), a popular computational method in computational chemistry. The idea behind it is the distribution of electrons in a system, which is described by the density of electrons.

Using density-functional theory (DFT) computations, scientists can calculate and analyze the system's energy, structure, and properties, among other things. Using density-functional theory (DFT), one may learn a lot about the geometry, electronic energy, ionization potential, electron affinity, and vibrational frequencies of a material, among other basic features.

Chemical processes, molecular interactions, and material behavior under varied conditions can all be better understood and predicted with the use of density-functional theory (DFT). Finding a compromise between accuracy and computing cost, DFT's computational efficiency makes it ideal for studying complicated systems and phenomena.

The DFT investigations in this research were conducted using the Gaussian 06 program. Using the Molden program, the resultant geometries were displayed. Molecular mechanics, semi-empirical approaches, and density functional theory research all make use of Gaussian, a flexible computational chemistry software package. In this work, all the simulations were run using Gaussian-09 on supercomputer. There were primarily two phases to the DFT calculations:

- Geometry Optimization
- TDSCF Calculation

3.3.1 *Geometry Optimization*

By making adjustments to the system's modeled geometry, most notably the nuclear coordinates of atoms, the objective of geometry optimization is to decrease the molecule's energy. Using the B3LYP hybrid density functional method and 6-311G basis set all the modeled geometries are optimized.

3.3.2 *B3LYP functional*

The B3LYP (Becke, 3-parameter, Lee-Yang-Parr) functional is one of the most widely used density functional theory (DFT) functionals in computational chemistry because it is a hybrid functional, meaning it combines elements of both Hartree-Fock theory (HF) and DFT. Moreover, B3LYP has been extensively benchmarked against experimental data and higher-level theoretical methods, demonstrating good agreement with observed chemical phenomena in many cases. It can accurately predict a variety of molecular properties such as molecular geometries, bond energies, reaction energies, electronic spectra, and molecular orbitals. These predictions can provide valuable insights into chemical reactivity, reaction mechanisms, and spectroscopic properties, facilitating the interpretation of experimental data. B3LYP calculations are frequently used in materials science and catalysis research to design and optimize new materials with desirable properties or to understand the underlying mechanisms of catalytic reactions. Because of its exceptional ability to accurately predict molecular structures and several other characteristics, it has become the most famous and extensively used hybrid functional model [121].

3.3.3 *6-311G Basis set*

The basis set consists of two distinct parts: a smaller basis set (6-31G) for the inner-shell electrons and a larger basis set (6-311G) for the valence electrons. The 6-311G basis set includes polarization and diffuse functions in addition to the standard Gaussian functions. These additional functions allow for a more flexible description of electron density, particularly for systems with significant electron correlation effects or for properties involving diffuse orbitals (such as excited states or weak interactions). The 6-311G basis set is a commonly used basis set

in quantum chemistry calculations. It is specified for molecular electronic structure calculations, particularly within the framework of Hartree-Fock (HF) and Density Functional Theory (DFT).

3.3.4 *Time-Dependent Self-Consistent Field*

Time-Dependent Self-Consistent Field (TDSCF) is a method used in quantum chemistry to study electronic excitations and calculate properties related to transitions between electronic states. TDSCF provides a rigorous theoretical framework for describing excited states, taking into account the interaction between electrons in the excited state and the surrounding environment. This allows for accurate predictions of excitation energies, transition dipole moments, and other properties related to electronic excitations. TDSCF calculations can predict optical properties such as absorption spectra, fluorescence spectra, and phosphorescence spectra. By simulating the excited-state dynamics of molecules, TDSCF can provide insights into the mechanisms of photochemical reactions and guide experimental investigations.

3.4 Description of Structures:

Total of 16 geometries have been modeled for this study. For the easy in explanation each structure has been given name.

Mol 1 to Mol 5 are based on C60 attached group. Figure 3-2 shows the sketch of these molecules.

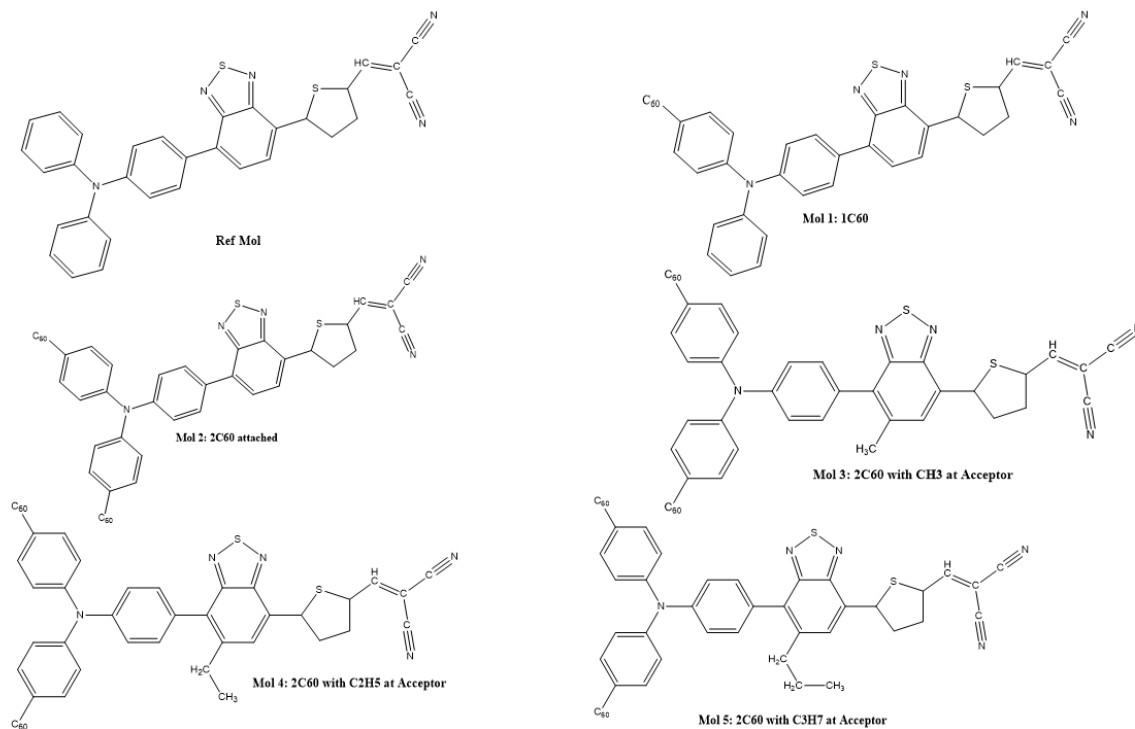


Figure 0-2: Structures based on C60 attached group

Mol 6 to Mol 10 are based on Pentacene attached group and Mol 11 to Mol 15 are based on 2H-benzo[cd]pyrene attached groups respectively. Their sketches are also shown in figure 3-3 and figure 3-4 separately.

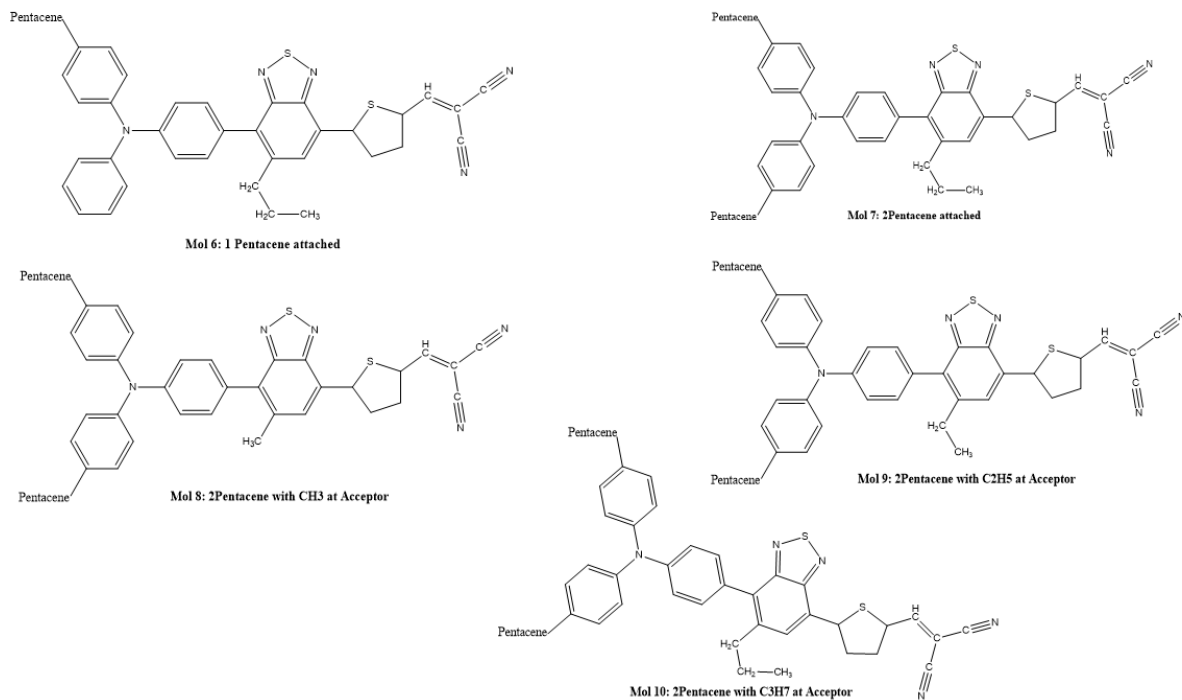


Figure 0-3: Structures based on Pentacene attached group

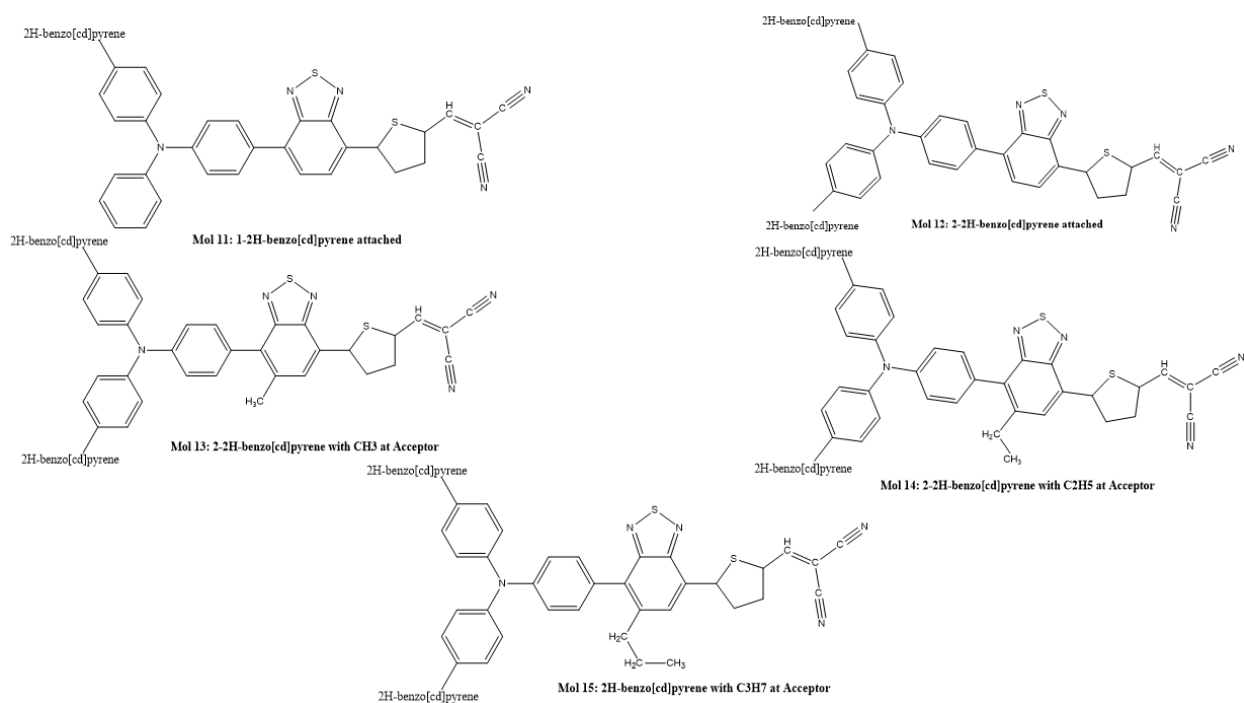


Figure 0-4: Structures based on 2H-benzo[cd]pyrene attached

Following is the table which describe the whole classification of structures.

Table 0-1: Classifications of Structures

Sr No.	Description	Structures-Attached with Basis Mol
1	Ref Mol	Reference
2	Mol 1	C60
3	Mol 2	2C60
4	Mol 3	CH3-2C60
5	Mol 4	C2H5-2C60
6	Mol 5	C3H7-2C60
7	Mol 6	Pentacene
8	Mol 7	2Pentacene
9	Mol 8	CH3-2PENTA
10	Mol 9	C2H5-2PENTA
11	Mol 10	C3H7-2PENTA
12	Mol 11	2H-benzo
13	Mol 12	2-2H-benzo
14	Mol 13	CH3-2H-benzo
15	Mol 14	C2H5-2H-benzo
16	Mol 15	C3H7-2H-benzo

CHAPTER 4: RESULTS

Density Functional Theory (DFT) study is performed to investigate the effect of fullerene and non-fullerene at the donor part of organic photovoltaic cell and the effect of alkyl group on the acceptor part using the hybrid functional DFT method B3LYP and the exchange-correlation functional basis set 6-311G (d).

4.1 Molecular Modeling

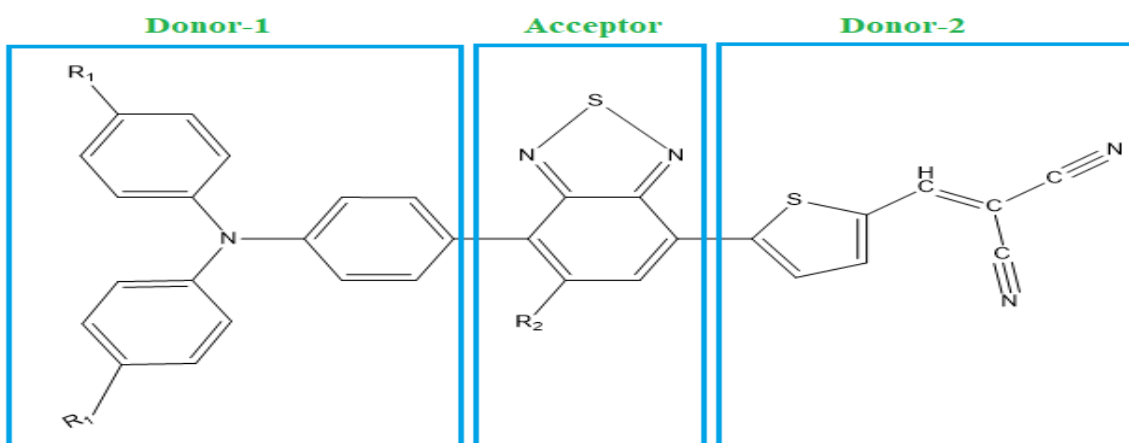
The reference geometry (Fig 4.1) of organic material used in organic photovoltaic cell was modeled using Gauss View. This is the Donor-Acceptor-Donor (D-A-D) structure, which can also be referred to as the D1-A-D2 structure for clarity.

This consists of two distinct donor units. Triphenylamine (TPA) has been identified as a good donor-1 substituent for enhancing photovoltaic performance and has a wide range of uses in organic photovoltaics. 2,5-dimethylthiophene with the chemical formula C_6H_8S , attached with two Cyanide groups is the second donor.

Figure 4-1: Structure of Basic Molecule

*R₁ = H, C₆₀, Pentacene, 2H-benzo[cd]pyrene

*R₂ = H, CH₃, C₂H₅, C₃H₇



4.2 Geometry optimization

The optimized geometry represented the most stable configuration of the molecule, identified by its lowest potential energy. Representing the lowest energy state achieved via geometry optimization, indicating the molecule's stable conformation.

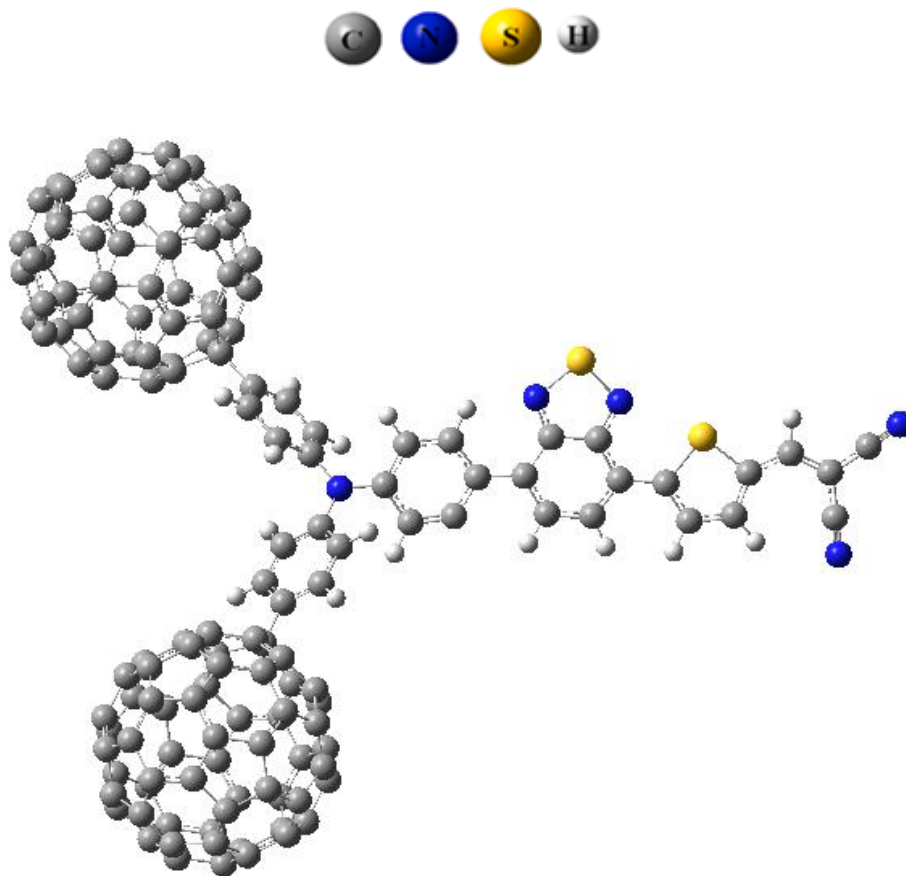


Figure 4-2: Optimized Structure of C60 attached molecule

To improve the functioning of reference molecule of the organic photovoltaic cell its triphenylamine (TPA) donor part is substituted with aromatic groups like C60, Pentacene, and 2H-benzo[cd]pyrene. Also, the effect of alkyl chain on the acceptor part is investigated. All the model geometries, presented in Figures 3-2, 3-3, 3-4, and 3-5, were optimized using DFT methods.

According to the computational results, the relative energy increases to 18.3eV when single C60 molecule is attached with the TPA (Mol-1), however, the relative energy further increases to 34.2 eV with the addition of second C60 molecule (Mol-2) (Table 4-1, Figure 4-2). Now to optimize the impact of alkyl chain, methyl, ethyl and propyl molecules are attached with the molecule with two C60 groups. The relative formation energy further increases to 48.7, 48.9 and 51.7 eV, which shows that the attachment of methyl, ethyl or propyl (Mol-3, Mol-4 & Mol-5 respectively) needs the similar amount of energy.

Table 4-1 The Energy value of Optimized Geometries of C60

Sr No.	Description	Optimization Energy (eV)	Relative Energy (eV)
1	Ref Mol	-62589.80955	0.000
2	Mol 1	-124776.620	18.296
3	Mol 2	-186965.794	34.228
4	Mol 3	-188035.485	48.688
5	Mol 4	-189105.136	48.936
6	Mol 5	-190172.082	51.720

Almost similar trend was observed when pentacene is attached with the TPA of reference molecule. The relative energy increases to 32.6 and 65.1 eV with the addition of single or two pentacene (Mol-6 or Mol-7 respectively) (Table 4-2) whereas the addition of alkyl chains to the acceptor part increases the almost 14.5eV energy requirement (Mol-8, Mol-9 & Mol-10).

Table 4-2 The Energy value of Optimized Geometries of Pentacene

Sr No.	Description	Optimization Energy (eV)	Relative Energy (eV)
1	Ref Mol	-62589.80955	0.000
2	Mol 6	-85599.206	32.553
3	Mol 7	-108608.605	65.103
4	Mol 8	-109678.296	79.563
5	Mol 9	-110747.992	79.766
6	Mol 10	-111817.694	79.795

Similarly, when 2H-benzo[cd]pyrene is attached with the TPA of reference molecule, the relative energy rises to approximately 17.4 eV and 65.3 eV with the addition of single or two 2H-benzo[cd]pyrene (Mol-11 or Mol-12, Table 4-3). whereas the addition of alkyl chains to the acceptor part requires the almost 14.7eV relative energy (Mol-13, Mol-14 & Mol-15).

Table 4-3: The Energy value of Optimized Geometries of 2H-benzo[cd]pyrene

Sr No.	Description	Optimization Energy (eV)	Relative Energy (eV)
1	Ref Mol	-62589.80955	0.000
2	Mol 11	-82454.950	17.430

3	Mol 12	-102289.608	65.343
4	Mol 13	-103359.301	79.801
5	Mol 14	-104428.945	80.056
6	Mol 15	-105498.648	80.084

4.3 Electronic properties

The energy gap (Egap) between the LUMO and HOMO is what determines the electronic properties of molecules. Electronic characteristics benefit from lower E_{gap} values.

Understanding the electronic structure and reactivity of molecules requires a thorough knowledge of the HOMO and LUMO. Both of these orbitals play an important role in molecule's reactivity and its ability to undergo various chemical reactions, such as electron transfer, bond formation, or bond breaking. The frontier orbitals were given their name due to the fact that they make it possible to predict how a molecule will interact with other species. Given its name as the orbital possessing the greatest number of electrons, HOMO often functions as an electron donor for those electrons. LUMO, conversely, is the most innermost orbital where electrons are permitted to penetrate. Consequently, while the HOMO energy exhibits an inverse relationship with the ionization potential, the LUMO energy demonstrates an inverse correlation with the electron. The energy gap, which characterizes the structure's reactivity and stability, is the energy difference between the HOMO and LUMO orbitals. The lower the HOMO-LUMO energy gap, more is the reactivity of the molecule.

The computed results indicate that the HOMO-LUMO energy gap decreases from 1.89 eV to 0.31 eV when one C₆₀ is attached (Mol-1), however, it increases to 1.49eV with the addition of second C₆₀ molecule (Mol-2). The addition of methyl group at the acceptor part of Mol-2 (two C₆₀ molecules attached) decreases the HOMO-LUMO energy gap to 1.38 eV from 1.49 eV (Mol-3, Table 4-6). Whereas this energy gap further increases to 1.96 eV and 1.5eV with the addition of ethyl and propyl groups, respectively (Mol-5 & Mol-6) (Table 4-4). According to the computed results of HOMO-LUMO energy gap for this Group, it has been observed that although the addition of two C₆₀ molecules or alkyl groups (methyl & propyl only) decreases the HOMO-LUMO energy gap than the reference molecule, Mol-1 where single C₆₀ molecule is attached with the TPA without the attachment of alkyl groups at the acceptor part shows more acceptable results.

Table 4-4: HOMO-LUMO Energy values and Energy gap values of C60 structures

Sr. No.	Description	HOMO (eV)	LUMO (eV)	Energy Gap (eV)
1	Ref Mol	-5.5615	-3.6692	1.8923
2	Mol 1	-5.125	-4.814	0.311
3	Mol 2	-5.880	-4.385	1.495
4	Mol 3	-5.7533	-4.3745	1.3788
5	Mol 4	-5.7873	-3.8205	1.9668
6	Mol 5	-5.5509	-4.0504	1.5004

Table 4-5 shows the results of HOMO-LUMO energy gap when pentacene was attached with reference molecule. The computed results show that the HOMO-LUMO energy gap decreases from 1.89 eV to 1.29 eV when one pentacene is attached (Mol-6) with reference molecule, whereas it further decreases to 1.26 eV with the addition of second pentacene molecule (Mol-7). The addition of methyl group at the acceptor part of Mol-7 (two pentacene molecules attached) increases the HOMO-LUMO energy gap to 1.332eV from 1.26eV (Mol-8). Whereas this energy gap further increases to 1.35 eV and 1.337 eV with the addition of ethyl and propyl groups, respectively (Mol-9 & Mol-10) (Table 4-5). By comparing all outcomes of this group it has been observed that Mol-7 where two pentacene molecule are attached with the TPA without the attachment of alkyl groups at the acceptor part shows more acceptable results.

Table 4-5: HOMO-LUMO Energy values and Energy gap values of Pentacene attached structures

Sr No.	Description	HOMO (eV)	LUMO (eV)	Energy Gap (eV)
1	Ref Mol	-5.5615	-3.6692	1.8923
2	Mol 6	-4.976	-3.683	1.294
3	Mol 7	-4.969	-3.705	1.264
4	Mol 8	-4.9522	-3.6194	1.3328
5	Mol 9	-4.9519	-3.5993	1.3527
6	Mol 10	-4.9470	-3.6099	1.3372

Table 4-6 shows the results of HOMO-LUMO energy gap when 2H-benzo[cd]pyrene was attached with reference molecule. The computed results show that the HOMO-LUMO energy gap decreases from 1.89 eV to 0.409 eV when one 2H-benzo[cd]pyrene is attached (Mol-11) with reference molecule, however, it increases to 1.039 eV with the addition of second 2H-

benzo[cd]pyrene molecule (Mol-12). The addition of methyl group at the acceptor part of Mol-13 (two 2H-benzo[cd]pyrene molecules attached) increases the HOMO-LUMO energy gap to 1.09 eV from 1.04 eV. Whereas this energy gap further increases to 1.11 eV with the addition of propyl (Mol-15) but remained unaffected with the addition of ethyl groups, 1.09eV (Mol-14). By comparing all outcomes of this group it has been observed that Mol-11 where two 2H-benzo[cd]pyrene molecule are attached with the TPA without the attachment of alkyl groups at the acceptor part shows more satisfactory results.

Table 4-6: HOMO-LUMO Energy values and Energy gap values of 2H-benzo[cd]pyrene attached structures

Sr No.	Description	HOMO (eV)	LUMO (eV)	Energy Gap (eV)
1	Ref Mol	-5.5615	-3.6692	1.8923
2	Mol 11	-4.498	-4.089	0.4090
3	Mol 12	-4.702	-3.663	1.0392
4	Mol 13	-4.6793	-3.5908	1.0885
5	Mol 14	-4.6738	-3.5791	1.0947
6	Mol 15	-4.6866	-3.5805	1.1061

Comparing the results obtained from the geometry optimization of all the modelled geometries, Mol-1 to Mol-15, it has been observed that Mol-1 (one C60 attached with reference molecule) shows the best in comparison with others while the 2nd best suited molecule is Mol-11 when 2H-benzo[cd]pyrene is attached with 1st donor and possess the energy gap of 0.41 eV.

4.4 Electronic Transition and Absorption spectra

The Electronic transition data provides insights into the behavior of electrons within the organic material layers of the solar cell. By understanding the energy levels involved in electronic transitions, researchers can optimize the design and composition of OPV materials to maximize light absorption and electron movement, thereby enhancing the efficiency of solar energy conversion electronic transition data was obtained for all the modelled geometries. Because longer-wavelength radiation, like radio waves and microwaves, lacks the energy necessary to produce electricity in a solar cell, the 400-800 nm range is crucial for photovoltaic applications.

The theoretical absorbance λ_{max} (nm), excitation energy E_{tr} (eV), and oscillator strength (O.S.) were all calculated using B3LYP/ 6-311G method. As shown in Table 4-7, the excitation configuration was calculated.

Table 4-7: The Excitation Energy, Absorption λ_{max} (nm), Oscillator strength (O.S) of C60 structures

Sr No.	Description	Excitation Energy (ev)	Wavelength (nm)	Oscillator Strength
1	Ref Mol	0.9720	1275.5100	0.0004
2	Mol 1	0.125	9960.250	0.030
3	Mol 2	0.113	10982.700	0.025
4	Mol 3	1.0444	1187.1200	0.0022
5	Mol 4	1.0629	1166.4400	0.0017
6	Mol 5	1.0592	1170.5500	0.0005

The computed electronic transition results indicate that the wavelength increases from 1275.5 nm to 9960.2 nm when one C60 is attached (Mol-1) with the reference molecule, however, it further increases to 10982.7 nm with the addition of second C60 molecule (Mol-2). However, the addition of methyl group at the acceptor part of Mol-2 (two C60 molecules attached) decreases the wavelength to 1187.1 nm from 10982.7 nm (Mol-3). This value further decreases to 1166.4 nm and 1170.5 nm with the addition of ethyl and propyl groups respectively (Mol-5 & Mol-6) (Table 4-7). Comparing the computed data, the values of wavelength for this Group shows, the addition of single C60 molecules and two C60 molecules increases the wavelength than the reference molecule, while attachment of alkyl groups decreases the wavelength. So when two C60 molecules are attached with the TPA without the attachment of alkyl groups at the acceptor part shows more favorable results. All values alkyl groups when attached with same donor part are closer to each other.

When the electronic absorption calculations were made for the Pentacene containing models, it has been observed that wavelength increases from 1275.5 nm to 6455.27 nm with the addition of one pentacene (Mol-6) in reference molecule, however, it further increases to the maximum value of 10826.57 nm with the addition of second pentacene molecule (Mol-7). The the addition of alkyl groups at the acceptor part of Mol-7 (two pentacene molecules attached) decreases the wavelength to ~ 2009 nm. The comparison of results of absorption spectra of this Group shows

almost similar behavior as for the group with C60. The addition of single pentacene molecules and two pentacene molecules increases the wavelength, while attachment of alkyl groups decreases the wavelength. So when two pentacene molecules are attached with the TPA without the attachment of alkyl groups at the acceptor part shows more favorable results (Table 4-8).

Table 4-8: The Excitation Energy, Absorption λ_{\max} (nm), Oscillator strength (O.S) of Pentacene attached structures

Sr No.	Description	Excitation Energy (ev)	Wavelength (nm)	Oscillator Strength
1	Ref Mol	0.9720	1275.5100	0.0004
2	Mol 6	0.192	6455.270	0.073
3	Mol 7	0.115	10826.570	0.025
4	Mol 8	0.6170	2009.4300	0.0000
5	Mol 9	0.6170	2009.5400	0.0000
6	Mol 10	0.6171	2009.0600	0.0000

When the electronic absorption calculations were made for the model geometries with the 2H-benzo[cd]pyrene, results indicate that wavelength increases from 1275.5 nm (Ref Mol) to 8989.0 nm when one 2H-benzo[cd]pyrene is attached (Mol-11) whereas, it decreases to 4568.6 nm with the addition of second 2H-benzo[cd]pyrene molecule (Mol-12). On the other hand the addition of methyl, ethyl and propyl groups at the acceptor part of Mol-12 (two 2H-benzo[cd]pyrene molecules attached) decreases the wavelength to 1147.8 nm, 1407.9 nm and 1392.1 nm respectively (Mol 14, Mol-15 & Mol-16). On comparing the computed results of absorption spectra, it has been observed the addition of single 2H-benzo[cd]pyrene molecules and two 2H-benzo[cd]pyrene molecules increases the wavelength, while attachment of alkyl groups decreases the wavelength. So when single 2H-benzo[cd]pyrene molecules are attached with the TPA without the attachment of alkyl groups at the acceptor part shows more promising results.

Table 4-9: : The Excitation Energy, Absorption λ_{\max} (nm), Oscillator strength (O.S) 2H-benzo[cd]pyrene attached structures

Sr No.	Description	Excitation Energy (ev)	Wavelength (nm)	Oscillator Strength
1	Ref Mol	0.9720	1275.5100	0.0004
2	Mol 11	0.138	8989.010	0.034

3	Mol 12	0.271	4568.650	0.144
4	Mol 13	0.7094	1747.7800	0.0047
5	Mol 14	0.8806	1407.8900	0.0090
6	Mol 15	0.8906	1392.1400	0.0118

Comparing with the literature, it has been observed that the computed wavelengths ranging from 1392.14 to 10982.7 nm falls within the infrared (IR) part of the electromagnetic spectrum. So Mol 2 has the highest value of wavelength and least value of excitation energy. Therefore, Mol 2 where 2C60 molecules are attached with the TPA part of reference molecule without the attachment of any alkyl groups shows the favorable results.

4.5 Photovoltaic properties

By determining the open-circuit voltage V_{oc} (eV) and α (eV) of all structures, the photovoltaic performance of the compounds under study was assessed. At the open-circuit voltage, solar cells can potentially produce their maximum voltage in the absence of a load. These photovoltaic properties were calculated from the HOMO and LUMO energies of modeled geometries.

The experimental values of V_{oc} and α were determined by applying the formula 1 and 2 below,

$$V_{oc} = |E_{HOMO}(\text{donor})| - |E_{LUMO}(\text{acceptor})| - 0.3 \quad \text{formula-1}$$

$$\alpha = |E_{LUMO}(\text{acceptor})| - |E_{LUMO}(\text{donor})| \quad \text{formula-2}$$

A molecule's energy gap is typically proportional to the gap between the donor's HOMO and acceptor's LUMO.

4.5.1 V_{oc} :

V_{oc} is the highest voltage that a device can generate when it's not connected to any external load. In short, it is the voltage between the terminals of a solar cell or panel while no current flows through them.

An increased open-circuit voltage (V_{oc}) of a solar cell is generally beneficial in following way.

- Increased Efficiency
- Better Performance in Low Light Conditions
- Reduced Voltage Losses:

➤ Improved System Flexibility

4.5.2 α (ΔE)

In the context from OPV, this Optimal energy difference α (ΔE) is critical because it determines the driving force for charge transfer activities at the donor-acceptor interface. A larger α facilitates more effective charge transfer and enhances the driving force for photo generated electron transfer from the donor to the acceptor. This energy differential affects the voltage of the open circuit (V_{oc}) & the overall effectiveness of an organic solar cell.

The computed results indicate that the value of open circuit voltage V_{oc} , decreases from 1.56eV to 1.12 eV when one C60 is attached (Mol-1) with the reference molecule, whereas, it increases to the value of 1.78 eV with the addition of second C60 molecule (Mol-2). It has been observed that the addition of methyl and ethyl group at the acceptor part of Mol-2 (two C60 molecules attached) shows no significant increase in V_{oc} to 1.75 eV(Mol-3) and 1.78 eV (Mol 4) respectively. However, the addition of propyl group at the acceptor part of Mol-2 decreases the V_{oc} value to 1.55eV. Comparing the computed results obtained for the V_{oc} , it has been observed that the addition of two C60 molecules with TPA and with the attachment of methyl or ethyl group at acceptor part (Mol-4) shows the improved V_{oc} than the reference molecule (table 4-10).

Optimal energy difference α (ΔE) range from -1.14 eV to +0.12 eV indicates a significant variation in the energy gap between the HOMO and LUMO orbitals of the molecule. A negative ΔE implies that LUMO energy level is lower than the HOMO energy level, such negative values indicates the presence of electron-rich species or molecules with electron-donating groups. In these cases, the LUMO is more stabilized compared to the HOMO. A positive ΔE indicates a more typical scenario where the LUMO energy level is higher than the HOMO energy level. This is the usual case in most molecules. While Mol 14 has the maximum value of optimal energy difference α .

Table 4-10: Showing the relationship of HOMO, LUMO, energy gap, V_{oc} and α C60 structure

Sr No.	Description	E_{HOMO}	E_{LUMO}	E_{gap}	V_{oc}	α
		(eV)	(eV)	(eV)	(eV)	(eV)
1	Ref Mol	-5.5615	-3.6692	1.892	1.5615	0.031
2	Mol 1	-5.125	-4.814	0.311	1.1250	-1.114
3	Mol 2	-5.787	-3.824	1.962	1.7865	-0.124

4	Mol 3	-5.7533	-4.3745	1.3788	1.7533	-0.675
5	Mol 4	-5.7873	-3.8205	1.9668	1.7873	-0.120
6	Mol 5	-5.5509	-4.0504	1.5004	1.5509	-0.350

The V_{oc} and α results of pentacene containing geometry models indicate that the V_{oc} decreases from 1.56 eV to 0.97 eV when one pentacene is attached (Mol-6) and from 0.97 eV to 0.96 eV with the addition of second pentacene molecule (Mol-7). The addition of methyl, ethyl and propyl groups at the acceptor part of Mol-7 (two pentacene molecules attached) further decreases the value of V_{oc} to ~0.95 eV from the molecules, Mol-8, Mol-9 & Mol-10 (Table 4-11). According to the computed results, the values of V_{oc} for this Group shows that the addition of single pentacene molecules with TPA without the attachment of alkyl group at acceptor part shows the uppermost value among all (Table 4-11). So all these values are less than the reference molecule which does not fulfill the requirement. Optimal energy difference α (ΔE) range from -0.005 eV to +0.101 eV indicates a significant variation in the energy gap between the HOMO and LUMO orbitals of the molecule. Such a small negative energy difference could potentially hinder efficient charge separation and reduce device performance. However, it's worth noting that in some cases, even a small negative energy difference can still allow for charge transfer if other factors such as material morphology or interfacial properties are favorable. When the energy of the HOMO of the donor material is higher than the energy of the LUMO of the acceptor material (positive ΔE), it facilitates efficient electron transfer from the donor to the acceptor during exciton dissociation.

Table 4-11: Showing the relationship of HOMO, LUMO, energy gap, V_{oc} and α of Pentacene attached structures

Sr No.	Description	E_{HOMO}	E_{LUMO}	E_{gap}	V_{oc}	α
		(eV)	(eV)	(eV)	(eV)	(eV)
1	Ref Mol	-5.5615	-3.6692	1.892	1.5615	0.031
2	Mol 6	-4.976	-3.683	1.294	0.9764	0.017
3	Mol 7	-4.969	-3.705	1.264	0.9688	-0.005
4	Mol 8	-4.9522	-3.6194	1.3328	0.9522	0.081
5	Mol 9	-4.9519	-3.5993	1.3527	0.9519	0.101
6	Mol 10	-4.9470	-3.6099	1.3372	0.9470	0.090

The computed results of Voc and α for the 2H-benzo[cd]pyrene containing models indicate that the value of open circuit voltage decreases from 1.56eV to 0.49 eV when one 2H-benzo[cd]pyrene is attached (Mol-11) with the reference molecule, which increases to 0.70 eV with the addition of second 2H-benzo[cd]pyrene molecule (Mol-12). The addition of methyl, ethyl and propyl groups at the acceptor part of Mol-12 (two 2H-benzo[cd]pyrene molecules attached) further decreases the Voc value to ~0.68 eV (Mol-13, Mol-14 & Mol-15, Table 4-12). According to the computed results, the values of Voc for this Group shows that the addition of two 2H-benzo[cd]pyrene molecules with TPA without the attachment of alkyl group at acceptor part shows the uppermost value among all (table 4-12). So all these values are less than the reference molecule which is not considerable. Optimal energy difference α (ΔE) range from -0.389 eV to +0.121 eV comes when 2H-benzo[cd]pyrene is attached with reference molecule. A negative energy difference of this magnitude typically presents a more significant barrier to efficient charge separation and can lead to increased energy losses due to charge recombination.

Table 4-12: Showing the relationship of HOMO, LUMO, energy gap, Voc and α of 2H-benzo[cd]pyrene attached structures

Sr No.	Description	EHOMO	ELUMO	Egap	VOC	α
		(eV)	(eV)	(eV)	(eV)	(eV)
1	Ref Mol	-5.5615	-3.6692	1.892	1.5615	0.031
2	Mol 11	-4.498	-4.089	0.409	0.4983	-0.389
3	Mol 12	-4.702	-3.663	1.039	0.7021	0.037
4	Mol 13	-4.6793	-3.5908	1.0885	0.6793	0.109
5	Mol 14	-4.6738	-3.5791	1.0947	0.6738	0.121
6	Mol 15	-4.6866	-3.5805	1.1061	0.6866	0.120

The suggested Voc and α values examined of D-A-D materials for electron ejection, making them suitable for bulk heterojunction and increasing their potential for use in solar cell applications. The value of Voc in Table 4-12 depends on the donor's HOMO and the acceptor's LUMO. The range of the variable "Voc" is from 0.498 eV to 1.787 eV, with an average value of 1.1 eV. The range of the variable " α " is from -1.114 eV to +0.121 eV, with an average value of -0.129 eV.

So by analyzing all computed result the addition of two C60 molecules with TPA and with the attachment of ethyl group at the acceptor part (Mol-4) is more favorable.

CHAPTER 5: DISCUSSION

Researchers have invested a lot of money into studying solar energy because it is a sustainable and abundant source of power. One common approach is photovoltaic, which turn sunlight into usable electricity by means of the photovoltaic effect.

Donor acceptor donor (D-A-D) part of photovoltaic cells have been the main focus of research, with a great deal of attention paid to the properties of the Donor-1 unit, the Acceptor unit, and the Donor-2 unit. For this purpose, 16 number of geometries were modelled, computed, and analyzed using DFT methods. For modelling, a molecule “2-((5-(7-(4-(diphenylamino)phenyl)benzo[c][1,2,5]thiadiazol-4-yl)thiophen-2-yl)methylene)malononitrile” was taken as a reference material (Figure 5-1), where Triphenylamine (TPA) part act as a Donor-1, 4,7-dimethylbenzo[c][1,2,5]thiadiazole as an Acceptor, and 2,5dimethylthiophene as a Donor-2

part.

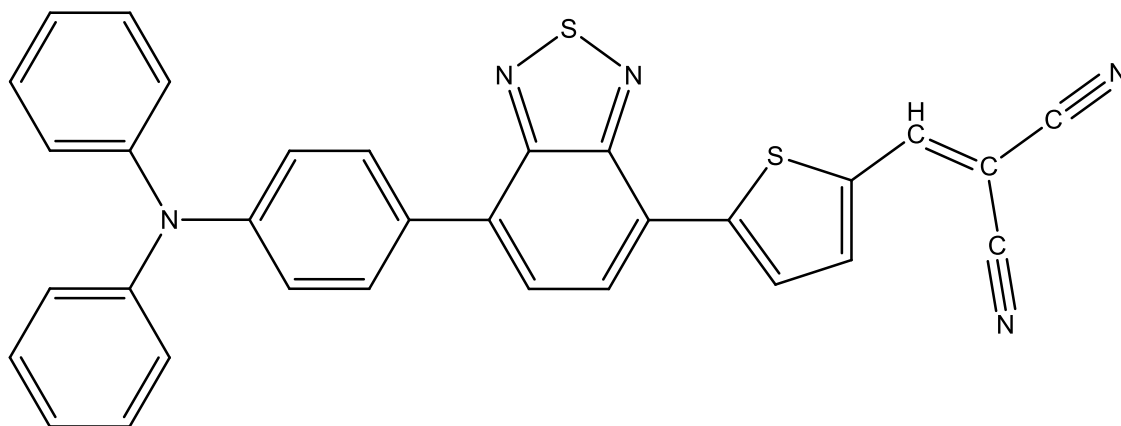


Figure 5-1: Reference Molecule

To understand the effect of aromaticity on the conductance, fullerene (C₆₀) and non-fullerene aromatic groups (Pentacene, 2H-benzo[cd]pyrene) were attached with the TPA-Donor-1 of the reference material. Certain aromatic compounds possess broad absorption spectra, extending the absorption range of the active layer in the OPV device. By attaching these compounds to the donor material, the device can harvest a wider range of solar radiation, thereby enhancing overall light absorption and increasing the photocurrent output.

The properties of D-A-D part of these modelled organic materials for OPV were characterized by:

- HOMO-LUMO Energy Gap
- Excitation energies
- Photovoltaic properties

Energy gap (E_{gap}) between HOMO and LUMO energy levels determines electronic properties of molecules. A smaller energy gap is required for the easy excitation of electron from HOMO to LUMO and allows for a larger built-in potential across the device, leading to higher voltages and thus potentially higher overall power output.

To evaluate the value of energy gap, we took a comparison by attaching single fullerene (C60) unit at donor-1 of a reference molecule resulting in decrease in energy gap (eV) ~ 0.31 eV than other two non-fullerene units. Similarly, 02 fullerene units were attached with the donor-1 and compared it with the attachment of 02 non-fullerene units at the same donor part. Now the results are different, the molecule where non fullerene unit (2H-benzo[cd]pyrene) was attached showed less energy gap value ~ 1.04 eV than the pentacene (non-fullerene) and C60 (fullerene unit). Then the electron donating alkyl groups (Methyl, Ethyl, Propyl) were attached with the acceptor unit of molecules with 02 fullerenes or 02 non fullerene units at donor-1 separately. The presence of electron-donating alkyl groups with acceptor part could lower the energy levels of the acceptor material, shifting its HOMO and LUMO energies towards higher electron affinity. However, the molecule where non fullerene unit (2H-benzo[cd]pyrene) was attached at donor-1 position and methyl was attached at acceptor unit showed less energy gap of ~ 1.09 eV than all other units. It was also observed that the attachment of different alkyl groups (Methyl, Ethyl, Propyl) does not show significant effect on the energy gap. So by comparing all the computed results we came to a point that attachment of fullerene unit at donor-1 when no alkyl group is attached with the acceptor part is most favorable to enhance the performance of organic photovoltaic application.

In OPVs, excitation energy is crucial because it determines the energy required to promote an electron from the valence band to the conduction band of the semiconductor material, initiating the generation of an electron-hole pair (exciton). This excitation occurs when the active layer of the solar cell absorbs photons from sunlight.

For a better solar cell application, its excitation energy should be minimum, which reflect that less energy is required to move an electron from HOMO to LUMO. As there is an inverse relationship between excitation energy and wavelength, the required wavelength should be greater for the excitation of electron in the PV cell. OPVs with materials that absorb light at longer wavelengths can capture a larger portion of the solar spectrum. This broad absorption range allows the solar cell to utilize a greater amount of incident sunlight, leading to higher overall efficiency. Photons with longer wavelengths carry lower energy compared to shorter-wavelength photons. Therefore, utilizing materials that absorb at high wavelengths ensures that these lower-energy photons are also converted into electricity, maximizing the photon harvesting capability of the solar cell.

According to our computational results, the minimum amount of excitation energy (~0.12eV) with wavelength 9960eV was required when a single fullerene unit was attached at donor-1 part of the reference molecule whereas the amount of energy increases when non-fullerene units were attached with the donor-1 part of the reference molecule. Similarly, with the attachment of two fullerene unit the amount of excitation energy ~0.11eV and wavelength 10982nm was observed which is better than the attachment of non-fullerene units. The effect of electron donating alkyl groups (Methyl, Ethyl, Propyl) with the acceptor unit of reference molecule was also studied and the results indicate that the alkyl groups does not show any substantial effect on the wavelength (range 1100-2000 nm) and excitation energy (range 0.61 -1.04 eV). So by comparing all computed results we came to a point that attachment of two fullerene unit at donor-1 when no alkyl group is attached with acceptor is most favorable to us. These results coincide with the results obtained from the HOMO-LUMO energy gap study.

Photovoltaic performance of the compounds under study could be assessed by open-circuit voltage V_{oc} (eV) and optimal energy difference α (ΔE). V_{oc} (eV) is the maximum voltage a solar panel can produce under standard test conditions (when no load is connected to it). A higher V_{oc} generally indicates a more efficient device, as it implies that a larger potential difference exists between the terminals of the solar cell, enabling higher power output for a given light intensity. A higher V_{oc} implies a more robust energy level alignment at the interfaces within the device, which can reduce charge carrier recombination and enhance device longevity.

The optimal energy difference α (ΔE) typically refers to the energy offset between HOMO of the donor material and LUMO of the acceptor material. α (ΔE) plays a critical role in determining the efficiency and performance of OPV devices. In general, a ΔE that is neither too small nor too large is considered optimal. If ΔE is too small, it may lead to inefficient charge separation and high recombination rates, resulting in decreased device performance. Conversely, if ΔE is too large, it can lead to increased energy losses and reduced photon harvesting efficiency.

The Voc and α (ΔE) values were calculated for all the optimized geometries with the fullerene, non-fullerene, and alkyl groups attached with the reference molecule. According to the computational results, where ethyl group is attached with the acceptor part and the two fullerene units at the donor-1 part of the reference molecule have the maximum Voc value, ~ 1.787 eV. The obtained results for the α (ΔE) indicates that when ethyl group is attached with acceptor in the presence of two non-fullerene (2H-benzo[cd]pyrene) units has the highest value of 0.121 eV. In the same way when single fullerene is attached with donor-1 in the absence of any alkyl group then α (ΔE) has the least value of -1.11 eV.

CHAPTER 6: CONCLUSION

In this work “DFT was performed to study the effect of fullerene and non-fullerene units on the donor part of reference material for the Organic Photovoltaic cell (Donor acceptor donor type of organic photovoltaic cell) with an additional focus on the effect of strategic modulation of attachment of methyl, ethyl and propyl groups with the acceptor one. Reference structure utilized for this study was the “2-((5-(7-(4-(diphenylamino)phenyl)benzo[c][1,2,5]thiadiazol-4-yl)thiophen-2-yl)methylene)malononitrile” for this purpose. The performance of designed D-A-D molecules was evaluated by calculating structural, electronic, optical, and absorption properties using DFT-B3LYP/6-311G levels of energy. According to computed data for the model geometries, attachment of single fullerene molecule with the TPA (donor part of, D-A-D material), when no alkyl group is attached with acceptor shows the least amount of energy gap value required to move an electron from HOMO to LUMO, possess highest wavelength and so the less amount of excitation energy, highest Voc value and the optimal α (ΔE) value. Summarizing the study, we conclude that attachment of single fullerene molecule with the TPA (donor part of, D-A-D material) without the addition of any alkyl group at acceptor part of D-A-D material is more beneficial for organic photovoltaic applications.

Future Perspective:

In future, further investigation of the structure-property relationships of donor materials in OPV cells through molecular engineering and design is demanding. This could involve modifying molecular structures, functional groups, or donor-acceptor interfaces to enhance device performance, stability, and scalability. Moreover, investigate the potential of emerging materials, such as organic-inorganic hybrid perovskites or 2D materials, as alternative donor materials in OPV cells. Use DFT-based screening to assess their suitability, stability, and performance compared to traditional organic donors. At the end apply computational modeling to optimize the overall device architecture and processing conditions of OPV cells for improved performance and manufacturability. This could include optimizing layer thicknesses, interfacial engineering, and device encapsulation strategies to enhance device efficiency, stability, and reliability.

REFERENCES

- [1] J. Conti, P. Holtberg, J. Diefenderfer, A. LaRose, J. T. Turnure, and L. Westfall, “International energy outlook 2016 with projections to 2040,” USDOE Energy Information Administration (EIA), Washington, DC (United States ...), 2016.
- [2] N. Amin, “Introduction of inorganic solar cells,” in *Comprehensive Guide on Organic and Inorganic Solar Cells*, Elsevier, 2022, pp. 57–63.
- [3] M. A. Green, “Corrigendum to ‘Solar cell efficiency tables (version 46)’ [Prog. Photovolt: Res. Appl. 2015; 23: 805–812],” *Progress in Photovoltaics: Research and Applications*, vol. 23, no. 9, pp. 1202–1202, 2015.
- [4] N. Saricifki, D. Braun, and C. Zhang, “VI Srdanov, AJ Heeger, G. Stucky and F. Wudl,” *Appl. Phys. Lett*, vol. 62, 1993.
- [5] J. Bernède, V. Jousseau, M. Del Valle, and F. Diaz, “From the organic electroluminescent diodes to the new organic photovoltaic cells,” *Current Trends in Polymer Sciences*, vol. 6, p. 135, 2001.
- [6] H. Becquerel, “Sur les radiations émises par phosphorescence (On the radiation emitted by phosphorescence),” *CR Acad. Sci*, vol. 122, pp. 420–421, 1896.
- [7] V. Andreev, “GaAs and High-Efficiency Space Cells, Chapter-1, Practical Handbook of Photovoltaics,” 2012.
- [8] The Nobel Prize, “The Nobel Prize in Physics 1921,” NobelPrize.org. [Online]. Available: <https://www.nobelprize.org/prizes/physics/1921/einstein/facts/>
- [9] “History,” Nokia Bell Labs. [Online]. Available: <https://www.bell-labs.com/about/history/>
- [10] I. Fraunhofer, “Photovoltaics Report.[Online] Available: <https://www.ise.fraunhofer.de/content/dam/ise/de/documents/publications/studies/Photovoltaics-Report.pdf>,” Accessed on: Jun, vol. 17, 2021.
- [11] T. Alves, J. P. N. Torres, R. A. Marques Lameirinhas, and C. A. F. Fernandes, “Different techniques to mitigate partial shading in photovoltaic panels,” *Energies*, vol. 14, no. 13, p. 3863, 2021.
- [12] V. M. Fthenakis and H. C. Kim, “CdTe photovoltaics: Life cycle environmental profile and comparisons,” *Thin Solid Films*, vol. 515, no. 15, pp. 5961–5963, 2007.

- [13] M. Rahman, S. Salehin, S. Ahmed, and A. S. Islam, "Environmental impact assessment of different renewable energy resources: a recent development," in *Clean Energy for Sustainable Development*, Elsevier, 2017, pp. 29–71.
- [14] M. Mottakin et al., "Design and Modelling of Eco-Friendly CH₃NH₃SnI₃-Based Perovskite Solar Cells with Suitable Transport Layers," *Energies*, vol. 14, no. 21, 2021, doi: 10.3390/en14217200.
- [15] I. Melo, J. P. Neto Torres, C. A. Ferreira Fernandes, and R. A. Marques Lameirinhas, "Sustainability economic study of the islands of the Azores archipelago using photovoltaic panels, wind energy and storage system," *Renewables: Wind, Water, and Solar*, vol. 7, no. 1, p. 4, Aug. 2020, doi: 10.1186/s40807-020-00061-8.
- [16] United Nations, "The 17 Sustainable Development Goals," United Nations. [Online]. Available: <https://sdgs.un.org/goals>
- [17] Z. M. Salameh, F. Dagher, and W. A. Lynch, "Step-down maximum power point tracker for photovoltaic systems," *Solar Energy*, vol. 46, no. 5, pp. 279–282, 1991.
- [18] K. Siri, V. Caliskan, C. Lee, and G. Agarwal, "Peak power tracking in parallel connected converters," presented at the [Proceedings] 1992 IEEE International Conference on Systems, Man, and Cybernetics, IEEE, 1992, pp. 1401–1406.
- [19] S. Kim, J. Lee, and B. Cho, "Large signal analysis of space aircraft power systems," presented at the Proc. IEEE 24th intersociety energy conversion engineering conference, 1989, p. 2873e80.
- [20] C. R. Sullivan and M. J. Powers, "A high-efficiency maximum power point tracker for photovoltaic arrays in a solar-powered race vehicle," presented at the Proceedings of IEEE Power Electronics Specialist Conference-PESC'93, IEEE, 1993, pp. 574–580.
- [21] A. Dasgupta, *Vertical Solar Panel: An Innovative approach Towards mitigating Energy Crisis situation of Urban India A Report*. 2022. doi: 10.37896/sr9.8/011.
- [22] M. K. A. Khan, S. Paul, S. R. Zishan, M. Abidullah, and S. Mahmud, "Design of a hybrid model of BPL electricity module and solar photovoltaic cell," *Int: J. of Sci. Eng. Research*, vol. 3, p. 12, 2012.
- [23] M. Imamzai, M. Aghaei, Y. H. M. Thayoob, and M. Forouzanfar, "A review on comparison between traditional silicon solar cells and thin-film CdTe solar cells," presented at the Proceedings of National Graduate Conference (Nat-Grad, 2012, pp. 1–5.
- [24] B. Williams et al., "Challenges and prospects for developing CdS/CdTe substrate solar cells on Mo foils," *Solar Energy Materials and Solar Cells*, vol. 124, pp. 31–38, 2014.
- [25] A. M. Bagher, M. M. A. Vahid, and M. Mohsen, "Types of solar cells and application," *American Journal of optics and Photonics*, vol. 3, no. 5, pp. 94–113, 2015.

- [26] P. N. Ciesielski et al., “Photosystem I–Based biohybrid photoelectrochemical cells,” *Bioresource technology*, vol. 101, no. 9, pp. 3047–3053, 2010.
- [27] O. Yehezkeli et al., “Integrated photosystem II-based photo-bioelectrochemical cells,” *Nature communications*, vol. 3, no. 1, p. 742, 2012.
- [28] Y. Goody, “Publications, presentations, and news database: Cadmium telluride,” National Renewable Energy Laboratory, 2009.
- [29] K. Zweibel, J. Mason, and V. Fthenakis, “A solar grand plan,” *Scientific American*, vol. 298, no. 1, pp. 64–73, 2008.
- [30] V. M. Fthenakis, “Life cycle impact analysis of cadmium in CdTe PV production,” *Renewable and Sustainable Energy Reviews*, vol. 8, no. 4, pp. 303–334, 2004.
- [31] C. Philibert et al., “Technology roadmap: solar photovoltaic energy,” International Energy Agency: Paris, France, 2014.
- [32] S. P. Philipps, A. W. Bett, K. Horowitz, and S. Kurtz, “Current status of concentrator photovoltaic (CPV) technology,” National Renewable Energy Lab.(NREL), Golden, CO (United States), 2015.
- [33] F. Andorka, “CIGS Solar Cells, Simplified,” *Solar Power World*. Archived from the original on, vol. 16, 2014.
- [34] M. L. Parisi, A. Sinicropi, and R. Basosi, “Life cycle assessment of thin film non conventional photovoltaics: The case of dye sensitized solar cells,” presented at the 25th International Conference on Efficiency, Cost, Optimization, Simulation and Environmental Impact of Energy Systems, 2012.
- [35] S. J. Moss and A. Ledwith, *Chemistry of the Semiconductor Industry*. Springer Science & Business Media, 1989.
- [36] D. J. Milliron, I. Gur, and A. P. Alivisatos, “Hybrid organic–nanocrystal solar cells,” *MRS bulletin*, vol. 30, no. 1, pp. 41–44, 2005.
- [37] S. E. Shaheen, D. S. Ginley, and G. E. Jabbour, “Organic-based photovoltaics: toward low-cost power generation,” *MRS bulletin*, vol. 30, no. 1, pp. 10–19, 2005.
- [38] B. R. Saunders and M. L. Turner, “Nanoparticle–polymer photovoltaic cells,” *Advances in colloid and interface science*, vol. 138, no. 1, pp. 1–23, 2008.
- [39] P. E. Shaw, A. Ruseckas, and I. D. Samuel, “Exciton diffusion measurements in poly (3-hexylthiophene),” *Advanced Materials*, vol. 20, no. 18, pp. 3516–3520, 2008.

- [40] M. G. Debijs, P. P. Verbunt, B. C. Rowan, B. S. Richards, and T. L. Hoeks, "Measured surface loss from luminescent solar concentrator waveguides," *Applied Optics*, vol. 47, no. 36, pp. 6763–6768, 2008.
- [41] P. Würfel and U. Würfel, *Physics of solar cells: from basic principles to advanced concepts*. John Wiley & Sons, 2016.
- [42] R. Blandford and M. Watkins, "This month in physics history: April 25, 1954: bell labs demonstrates the first practical silicon solar cell," *APS News*, vol. 18, no. 4, p. 2, 2009.
- [43] B. P. Rand, J. Genoe, P. Heremans, and J. Poortmans, "Solar cells utilizing small molecular weight organic semiconductors," *Progress in Photovoltaics: Research and Applications*, vol. 15, no. 8, pp. 659–676, 2007.
- [44] J. Song et al., "High-efficiency organic solar cells with low voltage loss induced by solvent additive strategy," *Matter*, vol. 4, no. 7, pp. 2542–2552, Jul. 2021, doi: 10.1016/j.matt.2021.06.010.
- [45] M. Vilckman et al., "Fully roll-to-roll processed organic top gate transistors using a printable etchant for bottom electrode patterning," *Organic Electronics*, vol. 20, pp. 8–14, 2015.
- [46] M.-E. Ragoussi and T. Torres, "New generation solar cells: concepts, trends and perspectives," *Chemical Communications*, vol. 51, no. 19, pp. 3957–3972, 2015.
- [47] C. W. Tang, "Two-layer organic photovoltaic cell," *Applied Physics Letters*, vol. 48, no. 2, pp. 183–185, 1986, doi: 10.1063/1.96937.
- [48] K. Petritsch, *Organic solar cell architectures*. na, 2000.
- [49] S. Sahare, "Enhancing the Photovoltaic Efficiency of a Bulk Heterojunction Organic Solar Cell," *Masters Theses & Specialist Projects*, 2016, Accessed: Jan. 01, 2024. [Online]. Available: <https://digitalcommons.wku.edu/theses/1609/>
- [50] G. Yu, J. Gao, J. C. Hummelen, F. Wudl, and A. J. Heeger, "Polymer photovoltaic cells: enhanced efficiencies via a network of internal donor-acceptor heterojunctions," *Science*, vol. 270, no. 5243, pp. 1789–1791, 1995.
- [51] C.-Y. Chang et al., "Combination of molecular, morphological, and interfacial engineering to achieve highly efficient and stable plastic solar cells," *Advanced Materials*, vol. 24, no. 4, pp. 549–+, 2012.
- [52] S. Zhang, Z. Chen, L. Xiao, B. Qu, and Q. Gong, "Organic solar cells with 2-Thienylmercaptan/AU self-assembly film as buffer layer," *Solar Energy Materials and Solar Cells*, vol. 95, no. 3, pp. 917–920, 2011.

- [53] N. Kaur, M. Singh, D. Pathak, T. Wagner, and J. Nunzi, "Organic materials for photovoltaic applications: Review and mechanism," *Synthetic Metals*, vol. 190, pp. 20–26, 2014.
- [54] N. B. McKeown, *Phthalocyanine materials: synthesis, structure and function*, no. 6. Cambridge university press, 1998.
- [55] Z. Hong, Z. Huang, and X. Zeng, "Investigation into effects of electron transporting materials on organic solar cells with copper phthalocyanine/C60 heterojunctions," *Chemical Physics Letters*, vol. 425, no. 1–3, pp. 62–65, 2006.
- [56] C. G. Claessens, D. González-Rodríguez, and T. Torres, "Subphthalocyanines: singular nonplanar aromatic compounds synthesis, reactivity, and physical properties," *Chemical reviews*, vol. 102, no. 3, pp. 835–854, 2002.
- [57] K. L. Mutolo, E. I. Mayo, B. P. Rand, S. R. Forrest, and M. E. Thompson, "Enhanced open-circuit voltage in subphthalocyanine/C60 organic photovoltaic cells," *Journal of the American Chemical Society*, vol. 128, no. 25, pp. 8108–8109, 2006.
- [58] K. Takahashi, T. Goda, T. Yamaguchi, T. Komura, and K. Murata, "Enhanced photocurrent in Al/porphyrin Schottky barrier cell with heterodimer consisting of metal-free porphyrin and zinc porphyrin," *The Journal of Physical Chemistry B*, vol. 103, no. 23, pp. 4868–4875, 1999.
- [59] T. Oku, T. Noma, A. Suzuki, K. Kikuchi, and S. Kikuchi, "Fabrication and characterization of fullerene/porphyrin bulk heterojunction solar cells," *Journal of Physics and Chemistry of Solids*, vol. 71, no. 4, pp. 551–555, 2010.
- [60] E. Perzon et al., "Design, synthesis and properties of low band gap polyfluorenes for photovoltaic devices," *Synthetic metals*, vol. 154, no. 1–3, pp. 53–56, 2005.
- [61] E. Ohno-Okumura et al., "Synthesis of subphthalocyanine derivatives and their characterization," *Dyes and pigments*, vol. 53, no. 1, pp. 57–65, 2002.
- [62] T. Ishii et al., "Fullerene C 60 exhibiting a strong intermolecular interaction in a cocrystallite with C 4 symmetrical cobalt tetrakis (di-tert-butylphenyl) porphyrin," *Journal of the Chemical Society, Dalton Transactions*, no. 20, pp. 2975–2980, 2001.
- [63] J. C. Hummelen, B. W. Knight, F. LePeq, F. Wudl, J. Yao, and C. L. Wilkins, "Preparation and characterization of fulleroid and methanofullerene derivatives," *The Journal of Organic Chemistry*, vol. 60, no. 3, pp. 532–538, 1995.
- [64] C. Liu, K. Wang, X. Gong, and A. J. Heeger, "Low bandgap semiconducting polymers for polymeric photovoltaics," *Chemical Society Reviews*, vol. 45, no. 17, pp. 4825–4846, 2016.

- [65] K. Müllen and W. Pisula, “Donor-Acceptor Polymers.,” *Journal of the American Chemical Society*, vol. 137 30, pp. 9503–5, 2015.
- [66] S. Günes, H. Neugebauer, and N. S. Sariciftci, “Conjugated polymer-based organic solar cells,” *Chemical reviews*, vol. 107, no. 4, pp. 1324–1338, 2007.
- [67] B. C. Thompson and J. M. J. Fréchet, “Polymer-fullerene composite solar cells.,” *Angewandte Chemie*, vol. 47 1, pp. 58–77, 2008.
- [68] F. Silvestri, M. D. Irwin, L. Beverina, A. Facchetti, G. A. Pagani, and T. J. Marks, “Efficient squaraine-based solution processable bulk-heterojunction solar cells,” *Journal of the American Chemical Society*, vol. 130, no. 52, pp. 17640–17641, 2008.
- [69] U. Mayerhöffer, K. Deing, K. Groß, H. Braunschweig, K. Meerholz, and F. Würthner, “Outstanding Short-Circuit Currents in BHJ Solar Cells Based on NIR-Absorbing Acceptor-Substituted Squaraines,” *Angewandte Chemie International Edition*, vol. 48, no. 46, pp. 8776–8779, 2009.
- [70] J. Mikroyannidis, D. Tsagkournos, S. Sharma, Y. Vijay, and G. Sharma, “Low band gap conjugated small molecules containing benzobisthiadiazole and thienothiadiazole central units: synthesis and application for bulk heterojunction solar cells,” *Journal of Materials Chemistry*, vol. 21, no. 12, pp. 4679–4688, 2011.
- [71] D. Marx and J. Hutter, *Ab initio molecular dynamics: basic theory and advanced methods*. Cambridge University Press, 2009.
- [72] B. J. Esselman and N. J. Hill, “Integration of computational chemistry into the undergraduate organic chemistry laboratory curriculum,” *Journal of Chemical Education*, vol. 93, no. 5, pp. 932–936, 2016.
- [73] F. Jensen, *Introduction to computational chemistry*. John wiley & sons, 2017.
- [74] D. C. Rapaport, *The art of molecular dynamics simulation*. Cambridge university press, 2004.
- [75] G. Bao and S. Suresh, “Cell and molecular mechanics of biological materials,” *Nature materials*, vol. 2, no. 11, pp. 715–725, 2003.
- [76] E. G. Lewars, “Introduction to Quantum Mechanics in Computational Chemistry,” in *Computational Chemistry: Introduction to the Theory and Applications of Molecular and Quantum Mechanics*, Springer, 2024, pp. 105–197.
- [77] A. North, D. t Phillips, and F. S. Mathews, “A semi-empirical method of absorption correction,” *Foundations of Crystallography*, vol. 24, no. 3, pp. 351–359, 1968.

- [78] M. Brandbyge, J.-L. Mozos, P. Ordejón, J. Taylor, and K. Stokbro, “Density-functional method for nonequilibrium electron transport,” *Physical Review B*, vol. 65, no. 16, p. 165401, 2002.
- [79] E. Chigo Anota, H. Hernández Cocolletzi, and E. Rubio Rosas, “LDA approximation based analysis of the adsorption of O₃ by boron nitride sheet,” *The European Physical Journal D*, vol. 63, pp. 271–273, 2011.
- [80] L. M. Fraas and M. J. O’Neill, “History of solar cell development,” in *Low-cost solar electric power*, Springer, 2023, pp. 1–12.
- [81] M.-S. Kim, *Understanding organic photovoltaic cells: Electrode, nanostructure, reliability, and performance*. University of Michigan, 2009.
- [82] K. Sivula and R. Van De Krol, “Semiconducting materials for photoelectrochemical energy conversion,” *Nature Reviews Materials*, vol. 1, no. 2, pp. 1–16, 2016.
- [83] M. Wolf and H. Rauschenbach, “Series resistance effects on solar cell measurements,” *Advanced energy conversion*, vol. 3, no. 2, pp. 455–479, 1963.
- [84] Macrotrends, “Crude Oil Prices - 70 Year Historical Chart,” Macrotrends. [Online]. Available: <https://www.macrotrends.net/1369/crude-oil-price-history-chart>
- [85] T. Markvart, *Solar electricity*, vol. 6. John Wiley & Sons, 2000.
- [86] M. D. Archer and R. A. Hill, *Clean Electricity from Photovoltaics*. in *Series on photoconversion of solar energy*. 2001. doi: 10.1142/p139.
- [87] A. Irfan and A. G. Al-Sehemi, “Quantum chemical study in the direction to design efficient donor-bridge-acceptor triphenylamine sensitizers with improved electron injection,” *Journal of molecular modeling*, vol. 18, pp. 4893–4900, 2012.
- [88] H. Hoppe and N. S. Sariciftci, “Organic solar cells: An overview,” *Journal of materials research*, vol. 19, no. 7, pp. 1924–1945, 2004.
- [89] S. D. Dimitrov and J. R. Durrant, “Materials design considerations for charge generation in organic solar cells,” *Chemistry of Materials*, vol. 26, no. 1, pp. 616–630, 2014.
- [90] T. Hori et al., “Solution processable organic solar cell based on bulk heterojunction utilizing phthalocyanine derivative,” *Applied physics express*, vol. 3, no. 10, p. 101602, 2010.
- [91] C. Du, J. Yu, J. Huang, and Y. Jiang, “Organic solar cells using Tin (II) phthalocyanine as donor material,” *Energy Procedia*, vol. 12, pp. 519–524, 2011.

- [92] G. Williams, S. Suttly, R. Klenkler, and H. Aziz, “Renewed interest in metal phthalocyanine donors for small molecule organic solar cells,” *Solar Energy Materials and Solar Cells*, vol. 124, pp. 217–226, 2014.
- [93] R. F. Salzman, J. Xue, B. P. Rand, A. Alexander, M. E. Thompson, and S. R. Forrest, “The effects of copper phthalocyanine purity on organic solar cell performance,” *Organic Electronics*, vol. 6, no. 5–6, pp. 242–246, 2005.
- [94] P. Kumar, K. Santhakumar, P.-K. Shin, and S. Ochiai, “Improving the photovoltaic parameters of organic solar cell using soluble copper phthalocyanine nanoparticles as a buffer layer,” *Japanese Journal of Applied Physics*, vol. 53, no. 1S, p. 01AB06, 2013.
- [95] N. Beaumont, S. W. Cho, P. Sullivan, D. Newby, K. E. Smith, and T. S. Jones, “Boron subphthalocyanine chloride as an electron acceptor for high-voltage fullerene-free organic Photovoltaics,” *Advanced functional materials*, vol. 22, no. 3, pp. 561–566, 2012.
- [96] Y. Ren et al., “Utilizing non-conjugated small-molecular tetrasodium iminodisuccinateas electron transport layer enabled improving efficiency of organic solar cells,” *Optical Materials*, vol. 129, p. 112520, 2022.
- [97] Q. Song, C. Li, M. Wang, X. Sun, and X. Hou, “Role of buffer in organic solar cells using C60 as an acceptor,” *Applied Physics Letters*, vol. 90, no. 7, 2007.
- [98] R. Pandey, A. A. Gunawan, K. A. Mkhoyan, and R. J. Holmes, “Efficient organic photovoltaic cells based on nanocrystalline mixtures of boron subphthalocyanine chloride and C60,” *Advanced Functional Materials*, vol. 22, no. 3, pp. 617–624, 2012.
- [99] F. Zhang et al., “Influence of PC60BM or PC70BM as electron acceptor on the performance of polymer solar cells,” *Solar Energy Materials and Solar Cells*, vol. 97, pp. 71–77, 2012.
- [100] Y. He, G. Zhao, B. Peng, and Y. Li, “High-yield synthesis and electrochemical and photovoltaic properties of indene-C70 bisadduct,” *Advanced Functional Materials*, vol. 20, no. 19, pp. 3383–3389, 2010.
- [101] L. Lu and L. Yu, “Understanding low bandgap polymer PTB7 and optimizing polymer solar cells based on it,” *Advanced Materials*, vol. 26, no. 26, pp. 4413–4430, 2014.
- [102] H. Yao, L. Ye, H. Zhang, S. Li, S. Zhang, and J. Hou, “Molecular design of benzodithiophene-based organic photovoltaic materials,” *Chemical reviews*, vol. 116, no. 12, pp. 7397–7457, 2016.
- [103] H. Pan et al., “Low-temperature, solution-processed, high-mobility polymer semiconductors for thin-film transistors,” *Journal of the American Chemical Society*, vol. 129, no. 14, pp. 4112–4113, 2007.

- [104] J. Hou et al., “Bandgap and molecular energy level control of conjugated polymer photovoltaic materials based on benzo [1, 2-b: 4, 5-b'] dithiophene,” *Macromolecules*, vol. 41, no. 16, pp. 6012–6018, 2008.
- [105] L. Huo and J. Hou, “Benzo [1, 2-b: 4, 5-b'] dithiophene-based conjugated polymers: band gap and energy level control and their application in polymer solar cells,” *Polymer Chemistry*, vol. 2, no. 11, pp. 2453–2461, 2011.
- [106] S. S. Reddy et al., “A new benzodithiophene based donor-acceptor π -conjugated polymer for organic solar cells,” *Macromolecular Research*, vol. 28, pp. 179–183, 2020.
- [107] J. Peet et al., “Efficiency enhancement in low-bandgap polymer solar cells by processing with alkane dithiols,” *Nature materials*, vol. 6, no. 7, pp. 497–500, 2007.
- [108] Z. Zhu et al., “Panchromatic conjugated polymers containing alternating donor/acceptor units for photovoltaic applications,” *Macromolecules*, vol. 40, no. 6, pp. 1981–1986, 2007.
- [109] I. Osaka, T. Abe, M. Shimawaki, T. Koganezawa, and K. Takimiya, “Naphthodithiophene-based donor–acceptor polymers: versatile semiconductors for OFETs and OPVs,” *ACS macro letters*, vol. 1, no. 4, pp. 437–440, 2012.
- [110] S. Steinberger et al., “ADADA-type oligothiophenes for vacuum-deposited organic solar cells,” *Organic letters*, vol. 13, no. 1, pp. 90–93, 2011.
- [111] M. Chen et al., “Ab initio theory and modeling of water,” *Proceedings of the National Academy of Sciences*, vol. 114, no. 41, pp. 10846–10851, 2017.
- [112] M. Yang, X. Chen, Y. Zou, C. Pan, B. Liu, and H. Zhong, “A solution-processable D–A–D small molecule based on isoindigo for organic solar cells,” *Journal of Materials Science*, vol. 48, pp. 1014–1020, 2013.
- [113] J. Zhang, G. Wu, C. He, D. Deng, and Y. Li, “Triphenylamine-containing D–A–D molecules with (dicyanomethylene) pyran as an acceptor unit for bulk-heterojunction organic solar cells,” *Journal of Materials Chemistry*, vol. 21, no. 11, pp. 3768–3774, 2011.
- [114] A. Yassin, P. Leriche, M. Allain, and J. Roncali, “Donor–acceptor–donor (D–A–D) molecules based on isoindigo as active material for organic solar cells,” *New Journal of Chemistry*, vol. 37, no. 2, pp. 502–507, 2013.
- [115] X. Wan, C. Li, M. Zhang, and Y. Chen, “Acceptor–donor–acceptor type molecules for high performance organic photovoltaics—chemistry and mechanism,” *Chemical Society Reviews*, vol. 49, no. 9, pp. 2828–2842, 2020.
- [116] J. E. Norton, J. r me Cornil, and V. Coropceanu, “Molecular Understanding of Organic Solar Cells: The Challenges,” *Acc. Chem. Res.*, vol. 42, no. 11, pp. 1691–1699, 2009.

- [117] T. Schlick, *Molecular modeling and simulation: an interdisciplinary guide*, vol. 2. Springer, 2010.
- [118] D. Dubbeldam, J. Vreede, T. J. Vlugt, and S. Calero, “Highlights of (bio-) chemical tools and visualization software for computational science,” *Current Opinion in Chemical Engineering*, vol. 23, pp. 1–13, 2019.
- [119] L. Radom, “John A. Pople (1925–2004),” *Nature*, vol. 428, no. 6985, pp. 816–816, Apr. 2004, doi: 10.1038/428816a.
- [120] A. Frisch, “gaussian 09W Reference,” Wallingford, USA, 25p, vol. 470, 2009.
- [121] A. C. Tsipis, “RETRACTED: DFT flavor of coordination chemistry,” *Coordination Chemistry Reviews*, vol. 272, pp. 1–29, 2014.